REPORT

Summary of Hydrogeology Existing Conditions

Meliadine Extension

Submitted to:

Agnico Eagle Mines Limited

Submitted by:

Golder Associates Ltd.

Suite 200 - 2920 Virtual Way, Vancouver, British Columbia, V5M 0C4, Canada

+1 604 296 4200

20136436-855-R-ExistingConditionsReport-Rev3

1 December 2021

Distribution List

1 e-copy Agnico Eagle Mines Limited

1 e-copy Golder Associates Ltd.

1 e-copy Nuqsana Golder

Table of Contents

TABLES

FIGURES

APPENDICES

1.0 INTRODUCTION

Agnico Eagle Mines Limited (Agnico Eagle) is proposing to expand the development at the Meliadine Gold Project (herein referred to as the Meliadine Extension or the Project), located approximately 25 km north from Rankin Inlet and 80 km southwest from Chesterfield Inlet in the Kivalliq Region of Nunavut. Baseline data have been collected in support of the environmental review to document existing conditions and to provide the foundation for a qualitative and quantitative assessment of Project operations and the extension of the mine development, to be evaluated in the Environmental Impact Statement (EIS) for the Project.

This report presents the results of the hydrogeology existing conditions for the Project. The Project includes open-pits and the Tiriganiaq underground development assessed through the 2014 FEIS (Agnico Eagle 2014a) plus new underground developments. The objective of the existing conditions report is to characterize the groundwater conditions in areas that will be potentially influenced by Mine development. The available data on existing conditions will be used to inform groundwater modelling, the effects assessment, water management plans and future groundwater effects monitoring.

2.0 HYDROGEOLOGY STUDY AREA

The hydrogeology study area is presented on Figure 1, relative to the existing and proposed underground developments and open pits. The study area is consistent with the regional study area from the 2014 FEIS (Agnico Eagle 2014a) and includes major lakes with interpreted open taliks, the largest of which is Meliadine Lake present to the east, north and west of the existing and proposed developments.

3.0 DATA REVIEW AND ANALYSIS

3.1 Lake Elevations and Bathymetry Data

Approximate elevations of lakes near the Project were obtained from the local topographic survey data, as provided by Agnico Eagle. Where local survey data were not available, approximate lake elevations were obtained from the National Topographic System (NTS) map sheets published by the Government of Canada.

As documented in the 2014 FEIS (Agnico Eagle 2014a), bathymetry data for lakes near the existing and proposed developments were obtained from data collected during field programs in 1997 and 1998 (RL&L 1999) and in 2001 (SD 7-1 2009 Aquatic Synthesis Report and DS 7-2 2011 Aquatics Baseline from the 2014 FEIS [Agnico Eagle 2014a]) and provided to Golder by Agnico Eagle.

3.2 Structural Geology Review

In the 2014 FEIS, three regional structures were considered in hydrogeological assessment (Lower Fault, Pyke Fault and North Fault). In support of the Project, Agnico Eagle completed a review of the structures near the proposed underground developments through examination of more recent drilling data, magnetic surveys breaks and interpretation of surficial lineaments. The objective of the review was to identify significant structures of potential enhanced permeability that may intersect the existing and proposed underground developments and be present within unfrozen bedrock. This review led to the identification of 17 faults that have been incorporated into the conceptual hydostratigraphy, in addition to the 3 regional faults (Lower Fault, Pyke Fault and North Fault) that were previously considered in the 2014 FEIS.

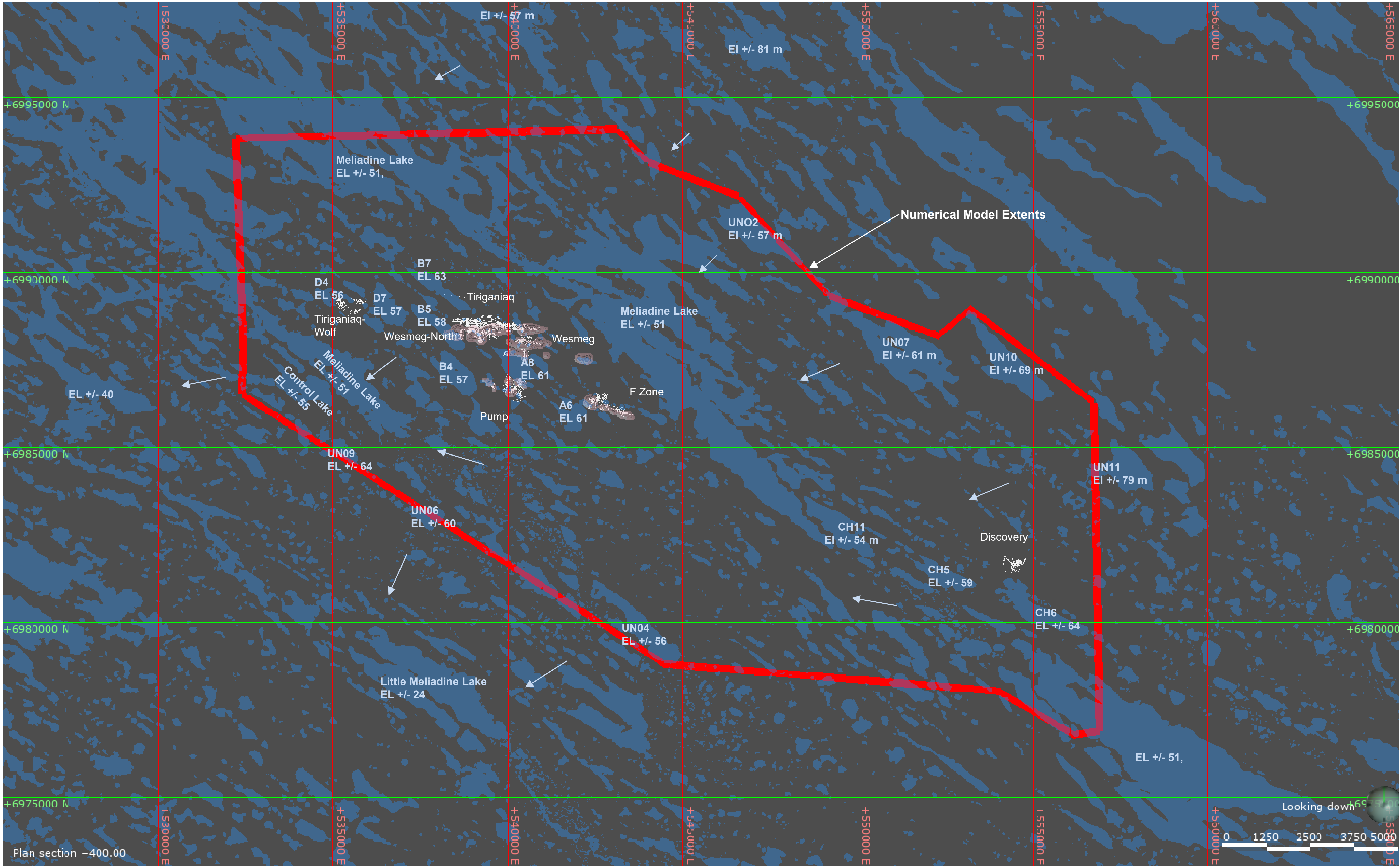

CLIENT

AGNICO EAGLE

CONSULTANT

GOLDER
MEMBER OF WSP

YYYY-MM-DD	2021-11-04
PREPARED	HG
DESIGNED	HG
REVIEWED	JL
APPROVED	DC

PROJECT

AGNICO EAGLE MINES LIMITED
MELIADINE EXTENSION
NUNAVUT

TITLE

HYDROGEOLOGY MODEL EXTENTS AND CONCEPTUAL REGIONAL GROUNDWATER FLOW DIRECTIONS

PROJECT NO.	PHASE	REV.	FIGURE
20136436	2300	3	1

The location of the faults identified by Agnico Eagle are presented on Figure 2 and Figure 3. The additional structures are generally located between the Lower Fault and Pyke Fault within the Mafic Volcanic Rock formations and range in thickness between 2 and 6 m based on information provided by Agnico Eagle. An exception is the KMS corridor, which is a wider zone of poor rock quality is generally located between the KMS fault and Lower Fault.

In the area of existing Tiriganiaq underground, there is a higher confidence in the structural interpretation and their presence as enhanced permeability features, particularly the RM175 and the KMS Fault Corridor. At the other underground developments, limited testing has been done to verify that the identified structures have enhanced permeability. In the absence of site-specific data, the structures have been conservatively assumed to have enhanced permeability relative to the surrounding bedrock, to extend several kilometres away from the underground development and to extend to a depth of approximately one kilometre (-1025 m elevation). The lateral extent of the KMS corridor is somewhat uncertain and was interpreted to encompass a zone of poor rock quality between the KMS Fault and Lower Fault. Based on input from Agnico Eagle geologists, a permeable 'skin' has been assumed along the lower fault of 15 to 20 m width to account for the potential extension of this corridor to the east and west.

3.3 Summary of Hydrogeological Testing

3.3.1 2009 and 2011 Testing Programs

Hydraulic test data from two field programs was available at the time of the 2014 FEIS (Agnico Eagle 2014a). A summary of the hydraulic testing results is summarized in Table 1 and the location of the boreholes tested are presented on Figure 4.

In 2009, three-single well response tests were conducted in 2 boreholes, as documented in Golder (2009 and 2011). Two of these tests were conducted in borehole GT09-19 within the talik of Lake B7 at vertical depths of about 40 metres below ground surface (mbgs) and 100 mbgs. The third test was conducted in borehole M09-860 from about 420 to 560 mbgs.

In 2011, seven single-well response tests were conducted at borehole M11-1257, located near Lake B5 to the west of Tiriganiaq Underground (Golder 2011). The first two tests were conducted using a packer at depths of 459 to 601 mbgs and 596 to 632 mbgs. Tests 3 through 7 at this location were conducted after the installation of a Westbay system in the borehole and were conducted in intervals 2 (602 to 613 mbgs), 2A (615 to 623 mbgs), 3 (574 to 585 mbgs), 4 (519 to 530 mbgs) and 5 (449 to 461 mbgs) respectively. The transmissivity and bulk hydraulic conductivity in the Westbay intervals were estimated from the pressure response collected by transducers within the sampling cylinders of the Westbay system.

In each of boreholes M09-860 and M11-1257, a single-well response test was conducted over an interval in deep bedrock that included the Lower Fault Zone. At M09-860 this included Test#1, which had an estimated transmissivity of 5×10^{-7} m^2/s. Assuming a five-metre-wide fault, this would indicate a Lower Fault hydraulic conductivity of 1×10^{-7} m/s. At M11-1257 this included Test #2, which had an estimated transmissivity of 1×10^{-7} m^2/s. assuming a five-metre-wide fault, this would indicate a Lower Fault hydraulic conductivity of 5×10^{-8} m/s. The hydraulic conductivity estimates of the bulk bedrock excluding the Lower Fault Zone ranged from 5×10^{-10} to 7×10^{-9} m/s.

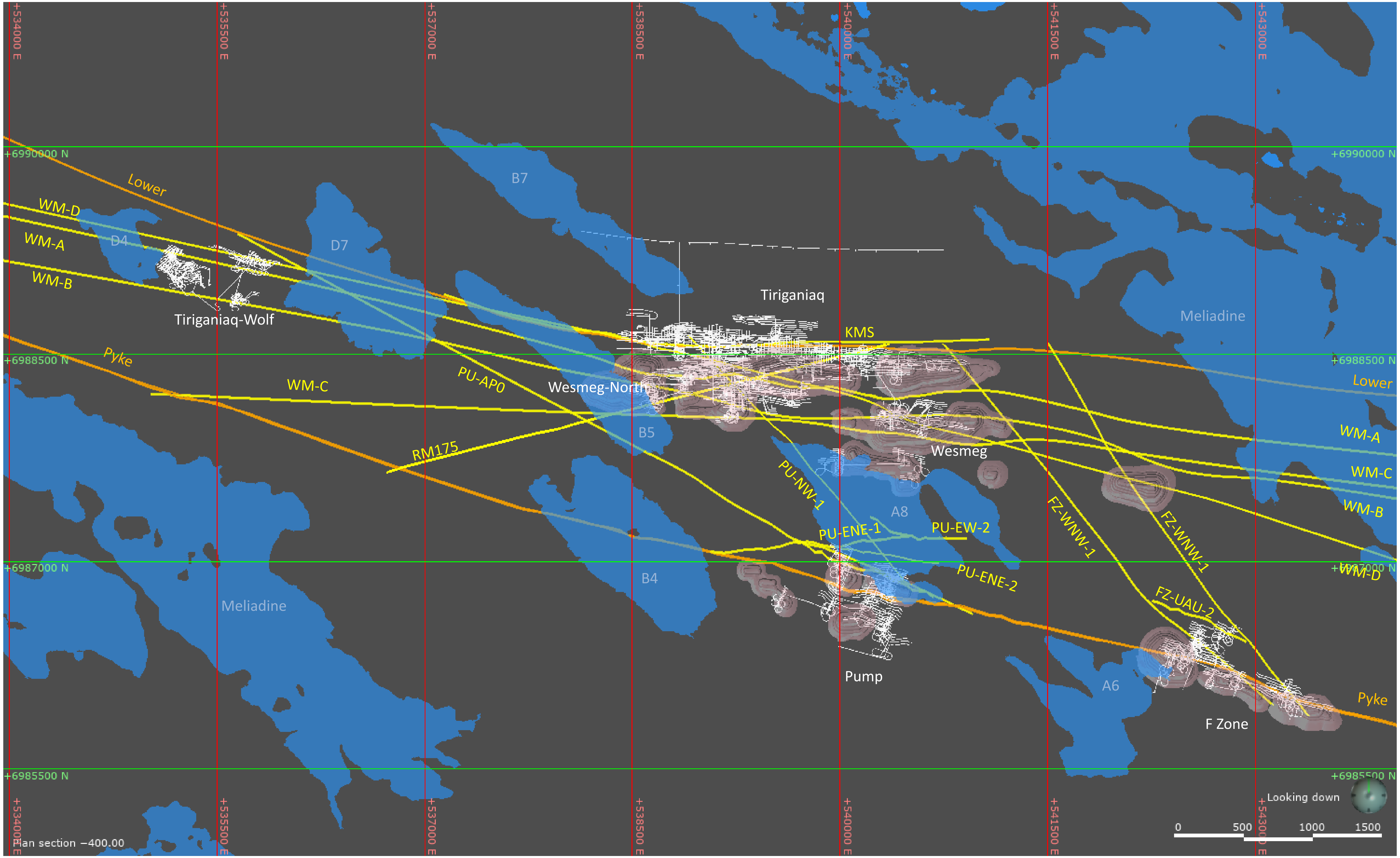

LEGEND

Inferred Lake with Open Talik

Regional Fault

Supplemental Faults Based on 2020 Agnico Eagle Review

Fault traces are shown for an elevation of -400 masl.

CLIENT

AGNICO EAGLE

CONSULTANT

GOLDER
MEMBER OF WSP

YYYY-MM-DD	2021-11-04
PREPARED	HG
DESIGNED	HG
REVIEWED	JL
APPROVED	DC

PROJECT

AGNICO EAGLE MINES LIMITED
MELIADINE EXTENSION
NUNAVUT

TITLE

STRUCTURES OF ENHANCED PERMEABILITY – MAIN AREA AND TIRIGANIAQ NORTH

PROJECT NO.	PHASE	REV.	FIGURE
20136436	2300	3	2

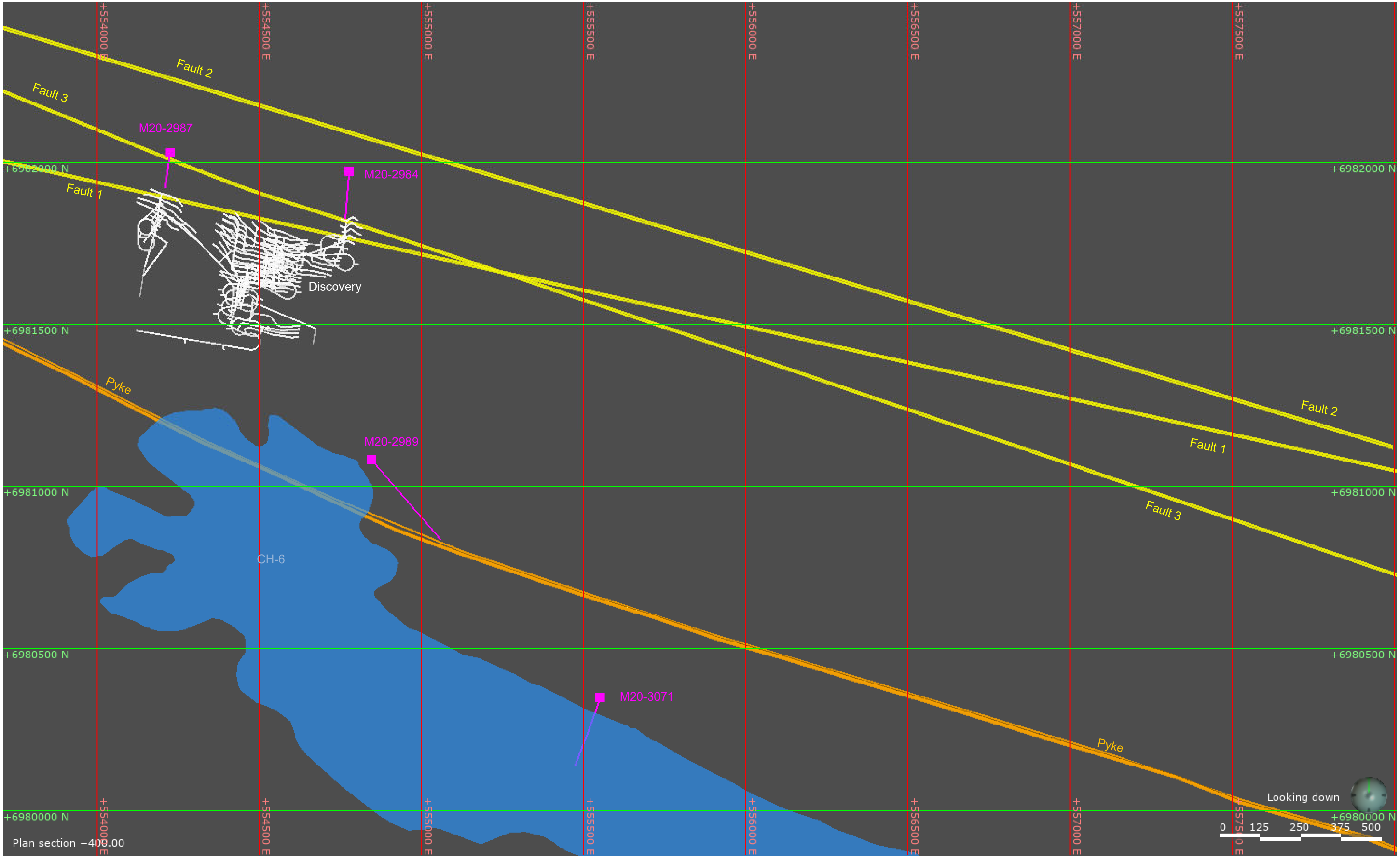

LEGEND

- Inferred Lake with Open Talik
- Regional Fault
- Supplemental Faults Based on 2020 Agnico Eagle Review
- Borehole Collar / Borehole Trace

Fault traces are shown for an elevation of -400 masl.

CLIENT: AGNICO EAGLE		PROJECT: AGNICO EAGLE MINES LIMITED MELIADINE EXTENSION NUNAVUT	
CONSULTANT: GOLDER MEMBER OF WSP	YYYY-MM-DD: 2021-11-04	TITLE: **STRUCTURES OF ENHANCED PERMEABILITY – DISCOVERY AREA**	
	PREPARED: HG		
	DESIGNED: HG		
	REVIEWED: JL	PROJECT NO. 20136436	PHASE 2300
	APPROVED: DC	REV. 2	FIGURE 3

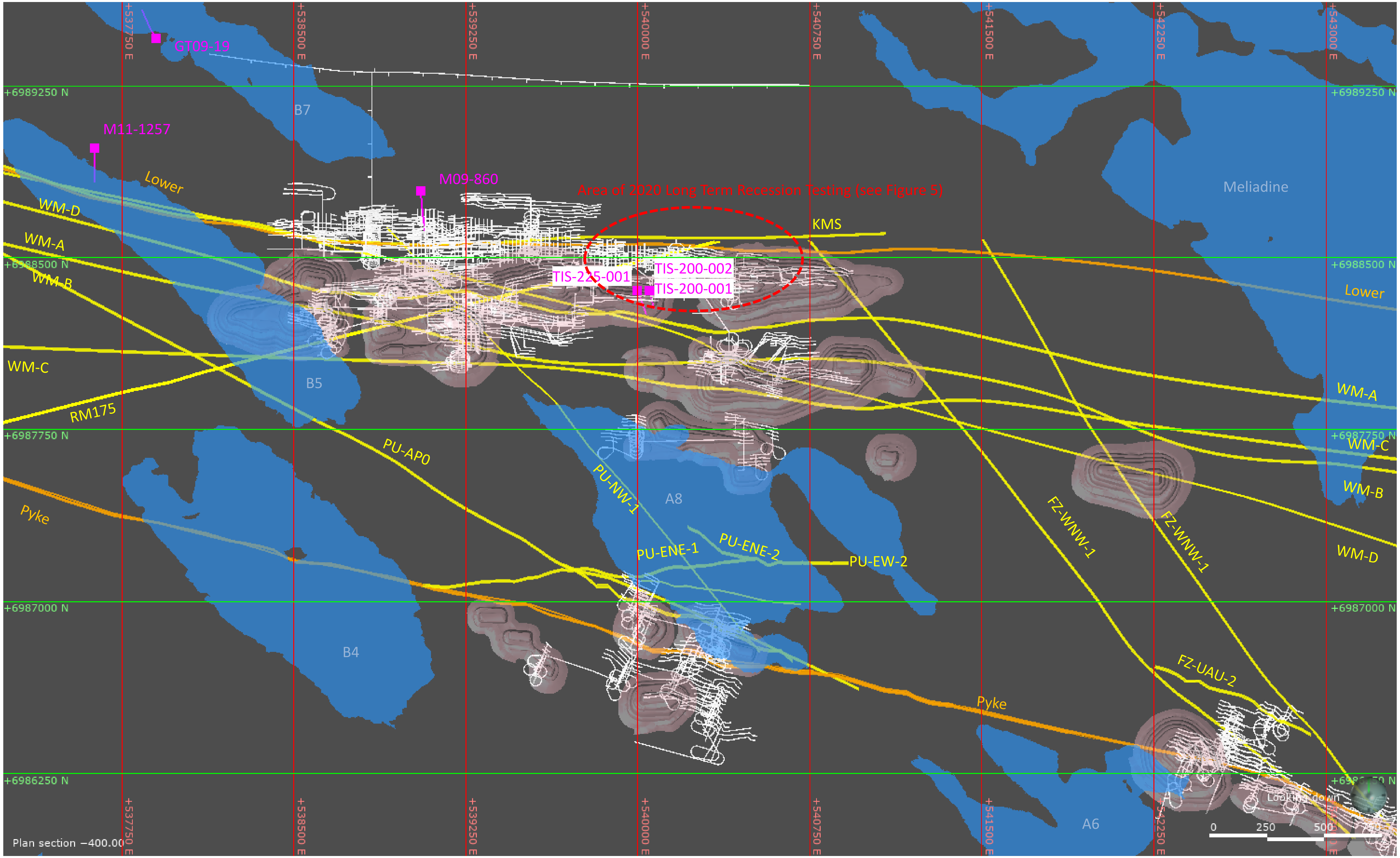

LEGEND

Inferred Lake with Open Talik

Regional Fault

Supplemental Faults Based on 2020 Agnico Eagle Review

Borehole Collar / Borehole Trace

Fault traces are shown for an elevation of -400 masl.

CLIENT	AGNICO EAGLE	PROJECT	AGNICO EAGLE MINES LIMITED MELIADINE EXTENSION NUNAVUT
CONSULTANT	GOLDER MEMBER OF WSP	TITLE	BOREHOLE LOCATIONS FOR HYDRAULIC TESTING AND GROUNDWATER SAMPLING – MAIN AREA
YYYY-MM-DD	2021-11-04	PROJECT NO.	20136436
PREPARED	HG	PHASE	2300
DESIGNED	HG	REV.	2
REVIEWED	JL	FIGURE	4
APPROVED	DC		

IF THIS MEASUREMENT DOES NOT MATCH WHAT IS SHOWN, THE SHEET SIZE HAS BEEN MODIFIED FROM: ANSI B

25 mm

Table 1: Summary of Available Hydraulic Testing Results – 2014 FEIS

Borehole	Test #	Interval Top (mbgs)	Interval Bottom (mbgs)	Interval Midpoint (mbgs)	West Bay Interval	Transmissivity (m^2/s)	Hydraulic Conductivity[1] (m/s)	Geology
GT09-19	1	27	56	42	-	1×10^{-7}	3×10^{-9}	Sam Formation
GT09-19	2	54	153	104	-	2×10^{-7}	2×10^{-9}	Sam Formation
M09-860	1	424	563	494	-	5×10^{-7}	3×10^{-9}	Sam Formation, Upper Oxide Formation, Wesmeg Formation, Lower Fault
M11-1257	7	449	461	455	Interval 5	3×10^{-8}	2×10^{-9}	Sam Formation
M11-1257	6	519	530	525	Interval 4	6×10^{-8}	5×10^{-9}	Sam Formation
M11-1257	5	574	585	580	Interval 3	8×10^{-8}	7×10^{-9}	Upper Oxide
M11-1257	4	615	623	619	Interval 2A	1×10^{-8}	1×10^{-9}	Wesmeg/Lower Fault
M11-1257	3	602	613	608	Interval 2	2×10^{-8}	2×10^{-9}	Tiriganiaq
M11-1257	2	596	632	614	-	1×10^{-7}	3×10^{-9}	Upper Oxide, Tiriganiaq, Wesmeg, Lower Fault
M11-1257	1	459	601	530	-	7×10^{-8}	5×10^{-10}	Sam Formation and Upper Oxide

1) Calculated based on estimated transmissivity and test interval length.

mbgs = metres below ground surface; m^2/s = square metres per second; m/s = metres per second.

3.3.2 2015 Underground Program

To improve the level of confidence in the predictions of groundwater inflow quantity and quality for the Tiriganiaq Underground, a hydrogeology gap analysis was completed by Golder in 2015 to 2016. Two independent technical advisors, Dr. Shaun K. Frape and Dr. Walter A. Illman (both from the University of Waterloo) provided advice and comments on the gap assessment.

The 2015 Underground Program (Golder 2016) was executed primarily within boreholes drilled from the Tiriganiaq underground development and consisted of the following hydraulic testing:

- 24 packer tests carried out over depth intervals ranging from 313 to 689 mbgs at three boreholes (TIS-200-001, TIS-200-002 and TIS-225-001)
- two flow recession pumping tests carried out from 327 to 593 mbgs and 592 to 689 mbgs below ground surface at TIS-200-002 and TIS-200-001 respectively, to characterize the storage properties and hydraulic conductivity of the bulk bedrock over a larger scale than can be tested by packer testing. During testing, one borehole acted as the pumping well and the other two boreholes as observation points.
- two injection tests carried out at TIS-200-002 to investigate the option of reinjecting water back into the formation.

A summary of the hydraulic test results is provided in Table 2, Table 3 and Table 4, with the location of the test holes presented on Figure 4.

Test 7 and 8 at TIS-200-001 intersected a potential fault, which is interpreted to be Fault A. The estimated transmissivity was between 1 x 10^{-6} m^2/s to 5 x 10^{-7} m^2/s over the tested intervals. Assuming a fault thickness of 5 m, this would indicate a hydraulic conductivity of between 1 x 10^{-7} m/s and 2 x 10^{-7} m/s. Analysis of the flow recession test in this borehole indicated a fault hydraulic conductivity of 4 x 10^{-8} m/s, which is slightly lower than that estimated from the single-well response test.

Test 6 and 7 at TIS-225-001 intersected a potential fault (likely Fault A), however the transmissivity was low (2 x 10^{-8} m^2/s to 5 x 10^{-8} m^2/s) and consistent with intervals with no identified fault. This may indicate the transmissivity of the faults is variable along its length, which is not unexpected.

At TIS-200-002, Test 5 is interpreted to have intercepted RM175. The transmissivity was estimated at 1 x 10^{-7} m^2/s. Assuming a fault thickness of 5 m, this would indicate a fault hydraulic conductivity of 2 x 10^{-8} m/s.

Results of both pumping tests indicate that the specific storage in the bedrock of the Wesmeg Formation to be on the order of 1 x 10^{-7} 1/m to 2 x 10^{-7} 1/m. At the time of the 2014 FEIS no site-specific information on the storage of the bedrock was available; therefore, in the FEIS, the specific storage was assumed to be 1 x 10^{-6} 1/m.

Table 2: Summary of Packer Tests – 2015 Underground Program

Borehole ID	Test Number	Interval Top (mbgs)	Interval Bottom (mbgs)	Interval Length (m vertical depth)	Interval Length (mah)	Structural Feature	Transmissivity (m^2/s)	Hydraulic Conductivity[1] (m/s)	Rock Type
TIS-200-001	Test 1	318.3	364.3	46.0	49.7	--	3×10^{-08}	5×10^{-10}	Mafic
TIS-200-001	Test 2	368.0	407.1	39.1	41.4	--	3×10^{-09}	$<1 \times 10^{-10}$	Mafic
TIS-200-001	Test 3	404.3	456.2	51.8	55.1	--	1×10^{-08}	2×10^{-10}	Mafic
TIS-200-001	Test 4	454.6	503.3	48.8	51.9	--	7×10^{-09}	1×10^{-10}	Mafic
TIS-200-001	Test 5	501.8	564.4	62.6	58.6	--	1×10^{-08} (a)	1×10^{-10} (a)	Mafic
TIS-200-001	Test 6	562.8	625.5	62.6	58.6	--	1×10^{-08} (a)	1×10^{-10} (a)	Mafic, Gabbro, Iron Formation, Ultramafic, Quartz Vein
TIS-200-001	Test 7	651.7	689.3	37.7	33.3	Joint, Fault A	5×10^{-07}	1×10^{-08}	Mafic, Gabbro, Iron Formation, Ultramafic
TIS-200-001	Test 8	623.9	689.3	65.4	57.9	Joint, Fault A	1×10^{-06}	1×10^{-08}	Mafic, Gabbro Iron formation, Ultramafic, Quartz ankerite Vein
TIS-225-001	Test 1	319.3	374.4	55.1	56.0	--	3×10^{-10}	$<1 \times 10^{-10}$	Mafic
TIS-225-001	Test 2	422.2	440.2	18.0	17.7	--	1×10^{-08}	7×10^{-10}	Mafic
TIS-225-001	Test 3	377.8	440.2	62.5	54.9	--	5×10^{-09}	$<1 \times 10^{-10}$	Mafic
TIS-225-001	Test 4	438.8	506.8	68.0	66.6	--	3×10^{-09}	$<1 \times 10^{-10}$	Mafic
TIS-225-001	Test 5	505.4	567.9	62.5	61.2	--	1×10^{-08}	1×10^{-10}	Mafic, Iron formation
TIS-225-001	Test 6	608.1	629.0	20.8	18.4	Fault A	5×10^{-08}	2×10^{-09}	Ultramafic, Iron formation
TIS-225-001	Test 7	563.7	629.0	65.2	57.8	Fault A	2×10^{-08}	3×10^{-10}	Iron formation, Ultramafic
TIS-225-001	Test 8	627.6	692.8	65.2	57.8	Joint	9×10^{-08}	1×10^{-09}	Ultramafic, Mafic
TIS-200-002	Test 1	316.2	326.0	9.8	10.0	Joint	3×10^{-07}	3×10^{-08} (b)	Mafic
TIS-200-002	Test 3	347.1	409.6	62.5	67.5	--	2×10^{-08}	3×10^{-10}	Mafic
TIS-200-002	Test 4	388.6	441.2	52.6	56.8	--	2×10^{-09}	$<3 \times 10^{-10}$	Mafic
TIS-200-002	Test 5	444.1	506.9	62.8	67.8	RM175	1×10^{-07}	2×10^{-09}	Mafic
TIS-200-002	Test 6	505.1	548.5	43.4	46.8	--	5×10^{-08}	1×10^{-09}	Mafic
TIS-200-002	Test 7	378.6	425.5	43.4	49.8	--	6×10^{-08}	1×10^{-09}	Mafic
TIS-200-002	Test 10	327.2	592.9	265.7	287.2	--	7×10^{-10}	$<1 \times 10^{-10}$	Mafic, Chert Iron formations
TIS-200-002	Test 11	592.3	689.3	97.1	104.9	Fault	4×10^{-8}	1×10^{-10}	Mafic, Chert Iron Formations

1) Calculated based on estimated transmissivity and test interval length; (a) Test could not be analyzed with analytical methods. Estimation only.

Table 3: Summary of Flow Recession Pumping Tests – 2015 Underground Program

Borehole ID	Interval Top (mbgs)	Interval Bottom (mbgs)	Interval Length (m vertical depth)	Interval Length (mah)	Hydraulic Conductivity (m/s)	Specific Storage (1/m)
TIS-200-002	327.2	592.9	265.7	286	2×10^{-10}	2×10^{-7}
TIS-200-001	592.3	689.3	97.1	104.9	4×10^{-8}	1×10^{-7}

Table 4: Summary of Injection Trial Results in TIS-200-022 – 2015 Underground Program

Test ID[b]	Cycle #	Average Pressure (Mpa)[a]	Average Flow Rate (L/min)[a]	Estimated Transmissivity (m^2/s)	Estimated Hydraulic Conductivity (m/s)
Test 1	1	3.2	0.4	8×10^{-08}	2×10^{-10}
	2	4.3	0.8	7×10^{-08}	2×10^{-10}
	3	4.8	0.7	6×10^{-08}	2×10^{-10}
	4	5.4	0.9	6×10^{-08}	2×10^{-10}
	5	5.9	0.9	5×10^{-08}	1×10^{-10}
	6	6.5	1.8	9×10^{-08}	2×10^{-10}
	7	7.0	2.7	1×10^{-07}	3×10^{-10}
	8	7.4	4.6	2×10^{-07}	5×10^{-10}
	9	7.6	7.0	3×10^{-07}	7×10^{-10}
	10	8.3	11.5	4×10^{-07}	1×10^{-9}
Test 2	1	3.3	1.1	2×10^{-07}	4×10^{-10}
	2	3.9	1.4	1×10^{-07}	4×10^{-10}
	3	4.7	1.8	1×10^{-07}	4×10^{-10}
	4	5.0	1.9	1×10^{-07}	3×10^{-10}
	5	5.6	1.8	1×10^{-07}	3×10^{-10}
	6	6.4	2.5	1×10^{-07}	3×10^{-10}
	7	7.0	3.4	1×10^{-07}	4×10^{-10}
	8	7.8	5.2	2×10^{-07}	5×10^{-10}
	9	8.3	8.8	3×10^{-07}	8×10^{-10}
	10	8.5	13.9	5×10^{-07}	1×10^{-9}

a) Average from last five minutes of the test. b) Tests conducted between approximately 330 and 730 mbgs.

3.3.3 2019-2020 Underground Program

In 2019 and 2020, Hydro-Resources Inc. on behalf of Agnico Eagle conducted short-term (few hours) and long-term (several days) recession tests from the Tiriganiaq underground in a series of 14 boreholes targeting the KMS corridor near the interpreted KMS fault and Lower Fault Zone (Figure 5). Data collection from the short-term recession tests were generally limited and did not provide reliable estimation of hydraulic conductivity: however, the long-term recession test conducted over approximately 72 hrs at WH350-157-D1 in July 2020 provided a good data set for estimation of the corridor hydraulic conductivity.

Hydro-Resources Inc. estimated transmissivity based on distance draw down analysis. Tested boreholes were both partially penetrating in some cases and extending past the outer limits of the corridor in others. Assuming an average interpreted corridor thickness of approximately 100 m, the hydraulic conductivity of the corridor was estimated from the provided transmissivity values to range between 2 x 10^{-7} m^2/s and 1 x 10^{-6} m^2/s with a geometric average of 4 x 10^{-7} m^2/s, indicating that the corridor is a zone of enhanced permeability.

Based on the collected pressure response data, a screening-level estimation of the hydraulic diffusivity was also calculated from the distance between the observation points and the pumped borehole, and the observed time for the first pressure response in the well. Hydraulic diffusivity gives a measure of diffusion speed of pressure disturbances in a groundwater system, and for consistent hydrostratigraphic units, the calculated diffusivity should be similar. Table 5 presents a summary of the calculated diffusivity, and indicates a wide range of hydraulic diffusivity, with values between <1 and 791 m^2/s. This variability indicates changes in the bedrock hydraulic properties between the pumped borehole and the observation points. For example, at PZ-ML375-194-D1-VW1 and VW3, the first response at the VW1 sensor was within 30 minutes whereas at VW3 it was after 85 m despite being relatively equal distance for the pumping well. This indicates that the KMS corridor may be composed of multiple discrete fractures with competent rock in between the fractures and that this compartmentalization results in heterogeneity in the hydraulic response. Given the complexity of the corridor, the hydraulic conductivity of the corridor will be evaluated further as part of numerical model calibration.

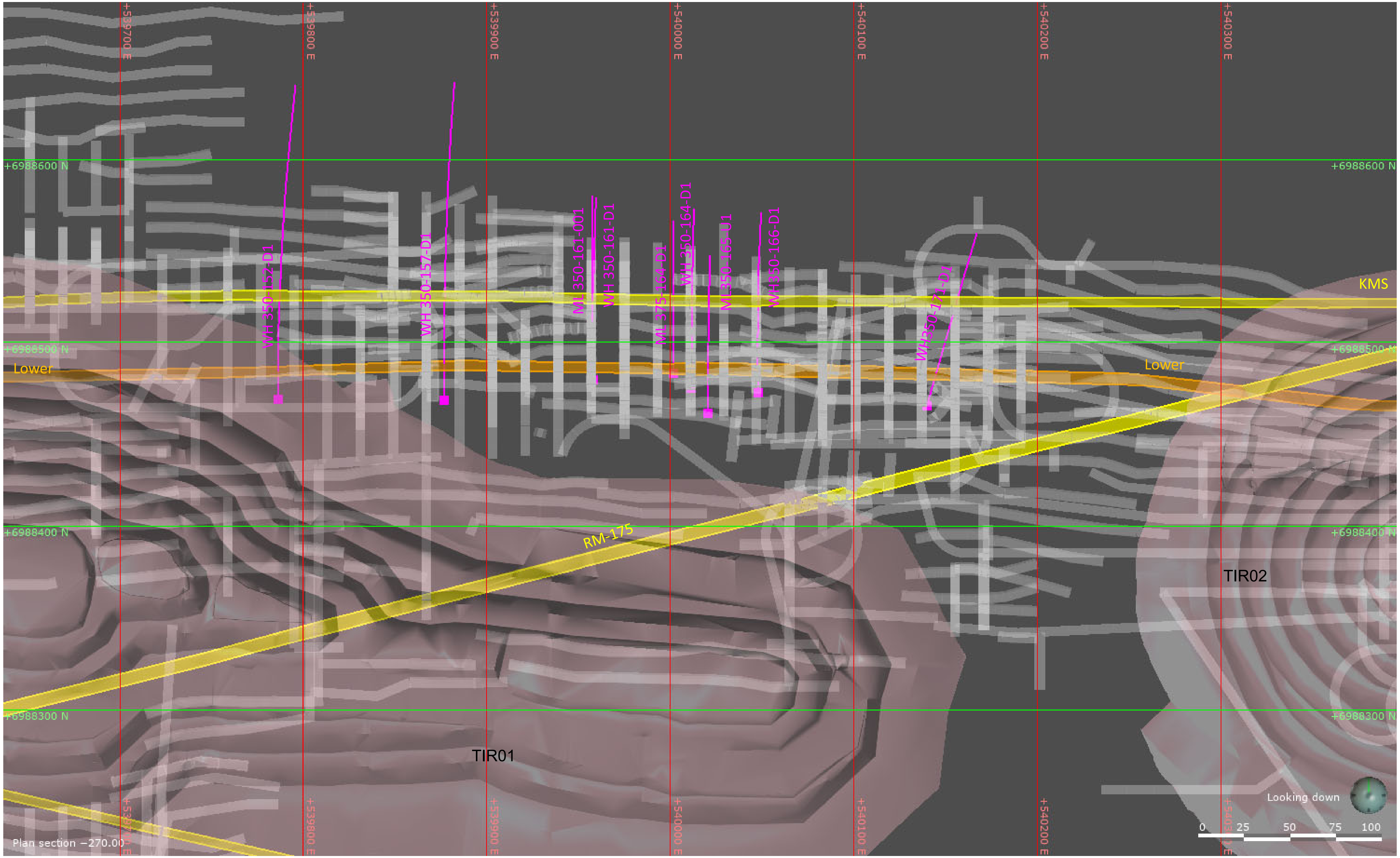

LEGEND

Regional Fault

Supplemental Faults Based on 2020 Agnico Eagle Review

Borehole Collar / Borehole Trace

Fault traces are shown for an elevation of -270 masl.

CLIENT

AGNICO EAGLE

CONSULTANT

GOLDER
MEMBER OF WSP

YYYY-MM-DD	2021-11-04
PREPARED	HG
DESIGNED	HG
REVIEWED	JL
APPROVED	DC

PROJECT

AGNICO EAGLE MINES LIMITED
MELIADINE EXTENSION
NUNAVUT

TITLE

BOREHOLE LOCATIONS FOR HYDRAULIC TESTING AND GROUNDWATER SAMPLING – KMS CORRIDOR

PROJECT NO.	PHASE	REV.	FIGURE
20136436	2300	2	5

Table 5: Summary of Estimated Hydraulic Conductivity and Diffusivity Values from Long Term Recession Test at WH350-157-D1

K (m/s)	Test Location	Observation Point												
	WH350-157-D1	WH350-161-D1	WH350-164-D1	ML350-165-U1	WH350-166-D1	PZ-WH350-152-VW1	PZ-WH350-152-VW2	PZ-WH350-152-VW3	PZ-ML17-350-161-VW1	PZ-ML17-350-161-VW2	PZ-WH350-171-D1-VW1	PZ-WH350-171-D1-VW2	PZ-ML375-164-D1-VW1	PZ-ML375-164-D1-VW3
Approximate Depth (mbgs)[b]	337	334	337	335	334	331	335	340	323	323	341	343	361	374
Hydraulic Conductivity (m/s)[(a)]	-	$3x10^{-7}$	$1x10^{-6}$	$7x10^{-7}$	$8x10^{-7}$	$3x10^{-7}$	$3x10^{-7}$	$3x10^{-7}$	$3x10^{-7}$	$3x10^{-7}$	$5x10^{-7}$	$5x10^{-7}$	$3x10^{-7}$	$2x10^{-7}$
Time to First Response (min)	NA	1	1	2	1	1	1	1	1	1	30	30	85	1
Distance to Pumping Well (m)	0	82	135	150	171	88	88	88	106	103	269	278	129	132
Calculated Diffusivity (m^2/s)	NA	545.5	410.7	73	790.7	323.8	310.2	310.2	72.2	68.2	10.3	11	0.8	190.5

a) Assuming an interpreted corridor thickness of 100 m. b) Approximate depth represents mid point of open borehole or elevation of vibrating wire sensor (VW1/VW2/VW3). Depth assumes a ground surface elevation of approximately 55 m.

3.3.4 2020 Discovery Testing

In May and June 2020, hydraulic testing was conducted in two boreholes in the proposed Discovery underground area. Seven tests were conducted at M20-2984 (DISCO-CONV-016) using packers at depths of between 5 and 499 mbgs and 5 tests were conducted at M20-2989 (DISCO-CONV-021-V2) using packers at depths of between 254 and 611 mbgs. A zone of enhanced permeability was interpreted in borehole M20-2984 between 512 and 524 mah, which has been interpreted to correspond to Fault 2 based fault locations provided by Agnico Eagle (Section 3.2). Hydraulic conductivity values calculated for the test intervals #2, 3, 4 and 7 that straddle the interpreted structure range from 6 x 10^{-8} to 4 x 10^{-7} m/s indicating moderate to low hydraulic conductivity. Transmissivity values calculated for these intervals (3 x 10^{-6} m^2/s to 6 x10^{-6} m^2/s,) demonstrate that despite the difference in test interval lengths the pressure responses in these tests are largely controlled by the properties of the enhanced permeability zone. Assuming a uniform thickness of 12 m, the hydraulic conductivity of the enhanced permeability zone was estimated to be between 3 x 10^{-7} m/s and 5 x 10^{-7} m/s, indicating a moderate hydraulic conductivity. A summary of the hydrogeological test results is summarized on Table 5 and documented in Golder (2021).

In August 2020, 13 single-well response tests were conducted at borehole M20-3071, located to the west of the proposed Discovery underground near Lake CH6 (Figure 3). The first 8 tests were packer tests completed between approximately 166.9 mbgs and 560.7 mbgs. The last five tests were conducted after the installation of a Westbay system in the borehole and were conducted at Ports 7, 8, 9, 10 and 11. The transmissivity and bulk hydraulic conductivity in these port intervals were estimated from the pressure response data collected by transducers within the sampling cylinders of the Westbay system. A summary of the hydrogeological test results is summarized on Table 6 and documented in Golder (2021c). Overall, hydraulic conductivity estimates ranged from less than 1 x 10^{-10} to 6 x 10^{-9} m/s.

Table 6: Summary of Hydraulic Test Results Near Discovery Underground – Fall of 2020

Borehole	Test Number	Interval Top (mbgs)	Interval Bottom (mbgs)	Interval length (mbgs)	Interval Length (mah)	Transmissivity (m^2/s)	Hydraulic Conductivity (m/s)	Geology
M20-2984	1[(b)]	256.4	388.1	131.7	142.4	6×10^{-7}[(b)]	1×10^{-9} [(b)]	Greywacke and Siltstone, Chert-Magnetite Iron Formation,
M20-2984	2[(b)]	397.9	485.4	87.4	94.5	6×10^{-6}	6×10^{-8}	Greywacke and Siltstone, Chert-Magnetite Iron Formation, Fault 2
M20-2984	3[(b)]	470.1	485.4	15.3	16.5	6×10^{-6}	4×10^{-7}	Greywacke and Siltstone, Chert-Magnetite Iron Formation, Fault 2
M20-2984	4[(b)]	389.6	485.4	95.8	103.5	6×10^{-6}	6×10^{-8}	Greywacke and Siltstone, Chert-Magnetite Iron Formation, Fault 2
M20-2984	5[(b)]	483.8	499.2	15.5	16.7	8×10^{-8}	5×10^{-9}	Gabbro, Greywacke and Siltstone, Chert-Magnetite Iron Formation
M20-2984	6[(c)]	4.6	499.2	494.6	534.6	[(c)]	[(c)]	Greywacke and Siltstone, Chert-Magnetite Iron Formation,
M20-2984	7	464.3	499.2	35.0	37.8	3×10^{-6}	8×10^{-8}	Gabbro, Greywacke and Siltstone, Chert-Magnetite Iron Formation, Fault 2
M20-2989	1[(c)]	254.5	535.7	281.2	303.9	[(c)]	[(c)]	Chloritic Siltstone and Greywacke, Altered Mafic Volcanics
M20-2989	2[(b)]	254.5	566.2	311.7	336.9	5×10^{-6}	2×10^{-8}	Chloritic Siltstone and Greywacke, Altered Mafic Volcanics
M20-2989	3[(b)]	376.6	566.2	189.6	204.9	2×10^{-6}	9×10^{-9}	Siltstone, Greywacke and Siltstone
M20-2989	4[(b)]	326.6	566.2	239.6	258.9	1×10^{-6}	4×10^{-9}	Altered Mafic Volcanics, Siltstone, Greywacke and Siltstone
M20-2989	5	418.2	610.6	192.4	207.9	7×10^{-7}	3×10^{-9}	Greywacke and Siltstone
M20-3071	1	171.9	213.8	41.9	44.6	5×10^{-8}	1×10^{-9}	Chloritic Siltstone and Greywacke
M20-3071	2	211.1	250.3	39.2	41.9	3×10^{-9}	$<1 \times 10^{-10}$	Chloritic Siltstone and Greywacke
M20-3071	3	246.5	286.4	39.9	42.0	3×10^{-7}	6×10^{-9}	Chloritic Siltstone and Greywacke
M20-3071	4	283.7	325.1	41.4	45.0	[(c)]	[(c)]	Chloritic Siltstone and Greywacke
M20-3071	5	325.5	360.9	35.4	38.6	$<2 \times 10^{-10}$	$<1 \times 10^{-10}$	Chloritic Siltstone and Greywacke
M20-3071	6	404.7	447.9	43.2	47.8	6×10^{-10}	$<1 \times 10^{-10}$	Chloritic Siltstone and Greywacke

Table 6: Summary of Hydraulic Test Results Near Discovery Underground – Fall of 2020

Borehole	Test Number	Interval Top (mbgs)	Interval Bottom (mbgs)	Interval length (mbgs)	Interval Length (mah)	Transmissivity (m^2/s)	Hydraulic Conductivity (m/s)	Geology
M20-3071	7	358.1	447.9	89.8	99.0	1×10^{-9}	$<1 \times 10^{-10}$	Chloritic Siltstone and Greywacke
M20-3071	8	445.2	561.0	115.8	129.0	7×10^{-9}	$<1 \times 10^{-10}$	Chloritic Siltstone and Greywacke, Chert-Magnetite Iron Formation
M20-3071	Port 11	243	273.3	30.3	32.6	2×10^{-8}	5×10^{-10}	Chloritic Siltstone and Greywacke
M20-3071	Port 10	274.1	291.7	17.6	19.0	7×10^{-8}	4×10^{-9}	Chloritic Siltstone and Greywacke
M20-3071	Port 9	292.5	310.0	17.5	18.9	7×10^{-9}	4×10^{-10}	Chloritic Siltstone and Greywacke
M20-3071	Port 8	310.8	326.9	16.1	17.5	6×10^{-8}[(a)]	3×10^{-9}[(a)]	Chloritic Siltstone and Greywacke
M20-3071	Port 7	327.7	382.5	54.8	60.0	1×10^{-9}[(a)]	$<1 \times 10^{-10}$[(a)]	Chloritic Siltstone and Greywacke

a) Low to moderate confidence in the result due to small magnitude of pressure change during the test.

b) Results are estimate only because the static conditions were not reached prior to test.

c) Results not reliable due to packer bypass observed during test.

d) Low to moderate confidence in the result due to small magnitude of pressure change during the test.

T = Transmissivity, K = Hydraulic Conductivity, mbgs = metres below ground surface, mah = metres along hole.

3.4 Groundwater Sampling

3.4.1 Data Collection

In support of the 2014 FEIS, groundwater sampling was conducted in the following locations to characterize the groundwater quality, in particular the salinity as indicated by total dissolved solids (TDS), as presented on Figure 6. This testing includes:

- one sample in borehole GT09-19 from 105 mbgs collected in 2009 (Golder 2009). This well is located within the talik of Lake B7.
- samples from eight intervals of the Westbay Monitoring Well M11-1157 (located near Tiriganiaq) at depths from 450 to 620 mbgs, below the base of the permafrost. Groundwater samples were collected from this well over four seasons, from 2011 to 2014 (Agnico Eagle 2014a; Agnico Eagle 2014b), with the 2014 sample being collected following the FEIS, with the 2014 sample being collected following the FEIS.

Additional data was collected from the Tiriganiaq underground between 2015 and 2020 and used to provide information on the lateral variability of groundwater quality (TDS) in the Tiriganiaq underground area. This data is included on Figure 5 and consists of:

- three groundwater samples collected by Agnico Eagle from seeps near the top of the cryopeg that were identified within the Tiriganiac underground development completed to November 2015.
- eight groundwater samples collected by Golder (2016) from borehole TIS-200-001 near the Tiriganiaq underground during a 96-hour pumping test carried from 630 to 725 m depth below ground, directly below the underground development.
- opportunistic groundwater samples collected by Agnico Eagle / Hydro-Resources Inc from diamond drill holes underground between 2016 and 2020 (located between approximately 230 and 450 m depth below ground).

In support of the Meliadine Extension, a second Westbay well (M20-3071) was installed near the proposed Discovery Underground and near the potential talik below CH6, as documented in Golder (2021c) and shown on Figure 5. Two ports were selected for development and sampling (Port 8 at approximately 310 to 326 mbgs and Port 4 at approximately 439 to 457 mbgs), with development and sampling methods and results documented in Golder (2021b). Port 8 sampling was selected to support assessment of water salinity in the talik between lake CH6 and the deeper regional groundwater flow of high salinity (below the regional permafrost). Port 4 sampling was selected to support assessment of water quality to be intercepted at the Discovery underground (i.e., it is at a similar elevation) the overall interpretation of regional water quality below the permafrost at similar depths At the time of this report, only Port 8 results are considered appropriate for estimating formation groundwater quality (Golder 2021b).

3.4.2 Groundwater Salinity Profile

In the Canadian Shield, concentrations of TDS in groundwater increase with depth, primarily in response to upward diffusion of deep-seated brines. The chemicals that contribute to TDS in shield brines are typically chloride and calcium, with sodium to a lesser degree, except in areas close to the ocean or areas that were submerged by oceans in the past (Séguin 1995) where sodium can be a significant contributor to TDS in groundwater. The major contributors to TDS in sea water are chloride and sodium.

The salinity of deep groundwater samples collected to date from Meliadine are at the high end of what has been observed at other sites in the Canadian Shield at corresponding depths (Frape and Fritz 1987; Stotler et al. 2012; Dominion 2014). The relatively high proportion of sodium relative to calcium in the groundwater sample likely indicates the presence of relict sea water in bedrock. It is known that this area was largely overlain by seawater during the last period of glaciation (Dyke et al. 2003).

Figure 6 presents the TDS profile with depth from sites in the Canadian Shield and that of the Meliadine groundwater samples. The Frape and Fritz dataset (1987) was developed based on chemical analyses of deep saline water collected by various investigators from several sites in the Canadian Shield. The Diavik dataset is based on site-specific data from Diavik, supplemented by information from the Lupin Mine site located about 200 km north of Diavik (Blowes and Logsdon 1997). The Meadowbank dataset (Golder 2004) was developed based on site specific data from the Meadowbank Mine site supplemented by the data sources discussed above (Frape and Fritz 1987; Blowes and Logsdon 1997). Of note is that the Meadowbank and Diavik datasets reflect talik groundwater rather than sub permafrost groundwater. The hydraulic connection with an overlying freshwater lake at these sites results in lower salinity at equivalent depths than has been observed below fully developed permafrost at the Project.

Although additional data has been collected to refine the profile, the interpreted TDS concentrations with depth is generally consistent with the TDS profile adopted in the FEIS (Agnico Eagle 2014a). Water quality in deep groundwater samplings suggest the salinity remains consistent with depth following the transition from near surface freshwater. Salinity concentrations in deep groundwater at Meliadine are approximately 1.6 times that of sea water (35 g/L).

Data collected from the underground diamond drill holes at Tiriganiaq are collected from depths between 230 and 450 m depth below ground. The circled tests on Figure 6 are inferred to be located above the zero-degree isotherm (base of permafrost) based on thermal modelling, and therefore within the cryopeg. TDS within the cryopeg may be elevated relative to groundwater in unfrozen rock at similar elevations due the preferential freezing of ‘fresher’ water and is similar to the assumed TDS below the regional permafrost (approximately 61,000 mg/L).

3.5 Permafrost Conditions

3.5.1 Depth to Permafrost and Lakes with Open Talik

Permafrost conditions at the time of the 2014 FEIS are described in SD 6-1 Permafrost Baseline Report in the 2014 FEIS (Agnico Eagle 2014a). Based on data at the time of the FEIS, the depth of permafrost was estimated to be on the order of 360 to 495 mbgs. Permafrost is defined as the zone extending from the bottom of the seasonally thawed layer (active layer) down to the 0-degree Celsius isotherm. The depth of the active layer ranges from approximately 1 to 3 m (Golder 2014).

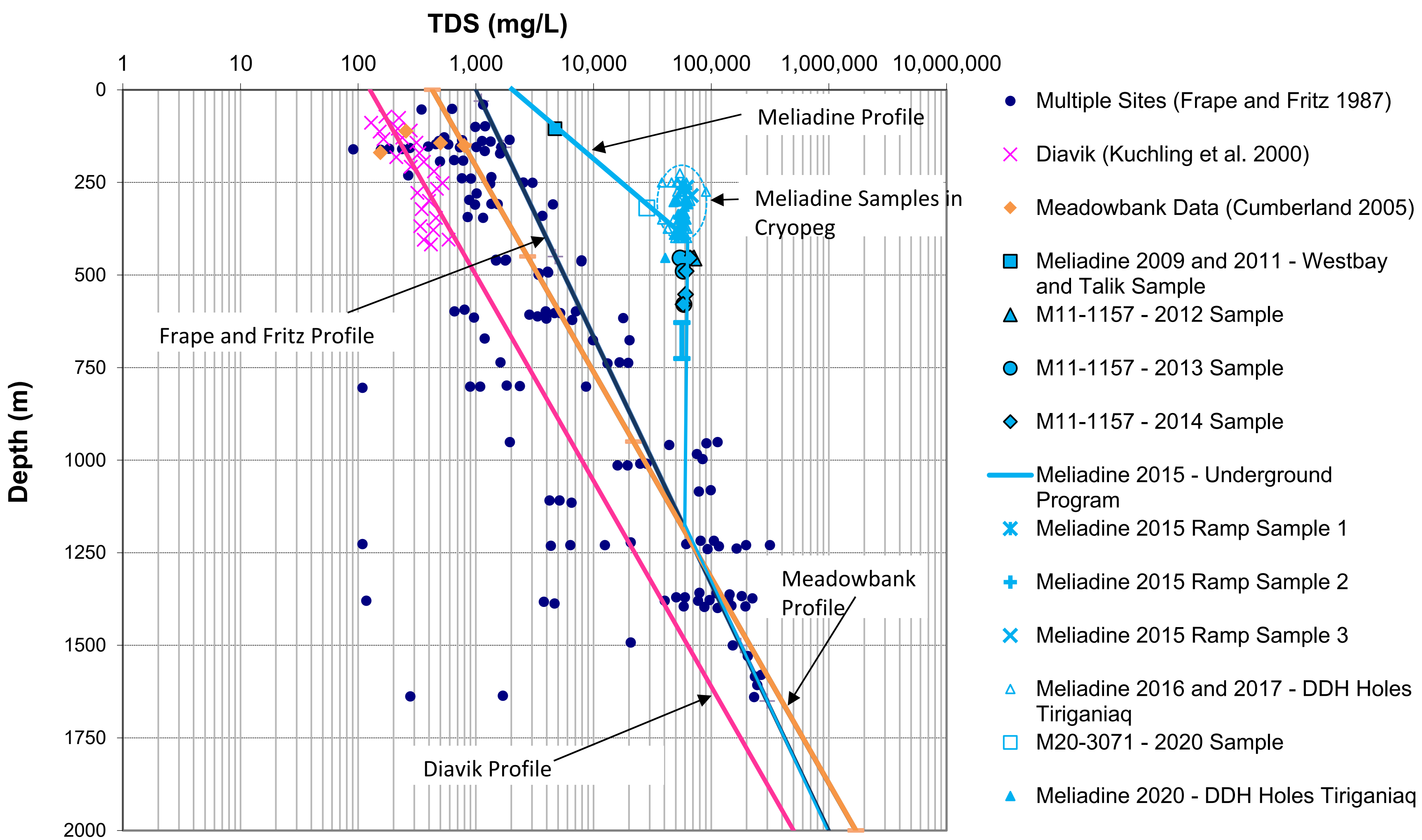

Notes:
TDS result plotted as midpoint of sample interval depth where applicable;
.

CLIENT
AGNICO EAGLE

CONSULTANT
GOLDER
MEMBER OF WSP

YYYY-MM-DD	2021-11-04
PREPARED	DH
DESIGN	–
REVIEW	JL
APPROVED	VJB

PROJECT
AGNICO EAGLE MINES LIMITED
MELIADINE EXTENSION
NUNAVUT

TITLE
GROUNDWATER SALINITY PROFILE WITH DEPTH

PROJECT No.	Phase	Rev.	Figure
20136436	2300	2	6

When the size of a lake is above a critical value, the talik beneath the lake will be an open talik, which connects to the deep groundwater flow regime beneath the permafrost (Golder 2014). Beneath smaller lakes, which do not freeze to the bottom over the winter, a talik bulb that is not connected to the deep groundwater flow system will form (closed talik). Analytical solutions were used by Golder (2014) in support of the 2014 FEIS to evaluate the critical lake sizes to support open talik in consideration of geothermal gradient, mean annual ground temperature, mean annual lake bottom temperature and bathymetry. The analysis indicated that taliks extending through the permafrost will exist beneath circular lakes having a minimum radius of approximately 290 to 330 m and beneath elongate lakes having a minimum half width of approximately 160 to 195 m, without considering lake terrace geometries. When terrace effects are included in the analysis, the critical radius for a circular lake increases to between approximately 305 to 485 m, and the critical half width for an elongate lake increase to between approximately 170 and 280 m. These were based on assumptions that the terrace is 25% to 75% of the total lake width or diameter, respectively. In consideration of the analysis, it was inferred in the 2014 FEIS that near the Tiriganiaq deposit (the location of the proposed single underground at the time), Meliadine lake, Lake B7, Lake B8 and Lake D7 will have open taliks connected to the deep groundwater flow regime. Lake A8 and Lake B5 are considered possible from the analytical assessment, but less certain.

In support of the Meliadine Extension, two-dimensional thermal modelling was completed (Golder 2021) to update the predicted depth to the base of permafrost in the study area, to assess the extent of lake taliks and to determine whether the proposed open pits and additional underground developments will remain within the permafrost limits. This approach was adopted given the number of proposed undergrounds and proximity of these undergrounds to lakes with potential open taliks. The 2D thermal modelling considered data from 10 active thermistors in the Project area, including three recently installed thermistors in the Discovery area (DC-16, DC-19-DC-21). The location of active thermistors installed at depths greater than 40 m within the vicinity of the area of interest is shown in Appendix A and summarized in Table 7.

Table 7: Thermistor Summary

Location	Thermistor	Collar Coordinates					Depth Below Ground Surface (m)
		Northing (m)	Easting (m)	Elevation	Inclination (°)	Azimuth (°)	
Tiriganiaq	GT09-19	6,989,458	537,899	63	51	123	152
	GT07-11	6,989,910	538,507	69	90	0	44
	GT07-10	6,988,805	538,506	69	90	0	44
F-Zone	GT09-07	6,986,260	542,429	60	60	74	130
	GT09-08	6,986,317	542,494	60	71	48	139
Discovery	DS09GT-03	6,981,625	554,379	72	67	54	129
	DS09GT-04	6,981,611	554,453	74	71	45	128
	DC-16[a]	6,981,980	554,770	67	70	179	475
	DC-19[a]	6,982,025	554,220	67	66	179	260
	DC-21[a]	6,981,071	554,846	70	60	140	572

a) Thermistors installed in 2020 and were still in the process of temperature stabilization at the time of this study.

Two-dimensional thermal models were prepared from 12 cross-sections throughout the study area and calibrated with thermistor data from the site and projected permafrost depths. Following completion of the 2D thermal models, results were used to create a three-dimensional (3D) block model for each of the three main areas of the Project:

- Tiriganiaq, F Zone, Pump and Wesmeg/Wesmeg-North deposits (Main Area)
- Discovery Area
- Tiriganiaq-Wolf Area

The 3D ground temperature blocks are intended to provide an overall view of the permafrost conditions with the Project areas. The methodology and results of the thermal modelling is presented in Golder (2021). Results of the thermal modelling indicated:

- open taliks are interpreted to be present beneath portions of each of the following lakes near the proposed open pits and undergrounds: Lake B4, Lake B5, Lake B7, Lake A6, Lake A8, Lake CH6 and Lake D4.
- The depth of the base of permafrost was between 285 and 430 m depth, with the interpreted depth dependent on the proximity to nearby lakes. Shallower depths are from locations near to lakes both with and without open taliks. The permafrost depth range predicted in the models is shallower than estimated in the 2014 Baseline Study, in which the depth of permafrost in the Project area was estimated to be between 360 m and 495 m.
- Based on permafrost depth limits and talik conditions predicted in this study, as well as locations and depths of open pits and undergrounds provided by Agnico Eagle, open pits in the F Zone, Pump and Discovery areas will be within permafrost. The depth of these pits range between 70 and 140 mbgs.
  The Wesmeg-North pit is planned to be about 130 m deep and is under a portion of Lake B5 where the models predict the existence of an open talik. This indicates the pit would operate in unfrozen ground and may intercept regional groundwater. One of the Wesmeg pits is planned to be about 120 m deep and is partially under the north side of Lake A8, where the models also predict the existence of an open talik. Therefore, this pit could also operate in partially unfrozen ground and intercept regional groundwater.

One historical thermistor in the FEIS (M98-195) is no longer monitored and was not considered in the assessment. Comparison of the historical measurements from M98-195 to the temperatures predicted by the 2D thermal modelling suggests the maximum permafrost depths in the Tiriganiaq area may be somewhat deeper than predicted by the thermal model. Overall, this would likely make the thermal model predictions conservative with respect to groundwater flow, with potentially more of the underground developments being located in frozen bedrock than is predicted by the thermal model at present.

3.5.2 Cryopeg Depth

Permafrost is defined as soil or rock where temperatures remain at or below 0°C for at least two consecutive years. The freezing temperature of water decreases when pressure and salinity increase. Consequently, within the permafrost unfrozen ground can be encountered at temperatures less than 0°C and in isolated pockets. These areas of unfrozen ground water are referred to cryopeg.

Groundwater inflows to the mine are expected to be negligible until mining extends below the depth of the permanently frozen portion of the permafrost: however, mine inflows can occur in the cryopeg where the ground is partially frozen. The depth at which these inflows may occur will depend on the thickness of the cryopeg.

Frozen permafrost depth and cryopeg thickness was estimated for Meliadine using the site-specific TDS/depth profile (Figure 6) and an iterative method used to estimate the frozen permafrost depth consists of the following steps:

- Step 1: Estimate groundwater salinity (TDS) from field measurements.
- Step 2: Calculate (approximate) the effect of salinity on freezing point depression (Temp1).
- Step 3: Cross-reference the calculated freezing point depression (Temp1) to estimate the frozen permafrost depth (D1) based on the ground temperature profile.
- Step 4: Estimate a revised salinity value (S2) from depth (D1) using the salinity depth profile.
- Step 5: Calculate a revised freezing point depression (T2) to estimate the frozen permafrost depth (D2).
- Repeat steps 4 to 6 until the values for the frozen depth permafrost converge.

Considering the temperature and TDS profile at the time of the FEIS, the frozen permafrost depth away from the lakes was estimated to be approximately 350 mbgs. Based on the updated groundwater quality data for the Project (Section 3.4) and the thermal modelling results, the frozen permafrost depth away from the lakes was estimated to be approximately 280 to 290 mbgs.

3.6 Tiriganiaq Groundwater Inflow Monitoring

Since the fourth quarter of 2015, groundwater inflow to the Tiriganiaq underground has been observed. Table 8 presents a summary of groundwater inflow estimates based on sump measurements and seepage surveys for the Tiriganiaq Underground, as provided by Agnico Eagle. The groundwater inflow ranges from 15 m^3/day in the fourth quarter of 2015, to more the recent 2020 monthly inflow estimates of between 190 and 295 m^3/day. The 2020 inflows are lower than the predicted inflows in the FEIS which ranged from 420 to 750 m^3/day in the first few years of mining to 640 to 970 m^3/day in later years. The lower than predicted inflows are to be expected because Agnico Eagle is mitigating the inflow of saline groundwater through active grouting as the development advances. Grouting was not considered in the FEIS groundwater inflow estimates.

Table 8: Measured Groundwater Inflows – Tiriganiaq

Month and Year	Estimated Average Monthly Inflow (m^3/day)
Q4 2015	15
January 2017	35
October 2018	155
November 2018	175
December 2018	200
2019	160 to 470*
2020	190 to 295*

* Peak monthly flows in 2019 and 2020 reflect periods where the boreholes were allowed to free drain into the underground as part of recession testing. These high inflows are not representative of typical inflows to the underground, which will be a calibration target for the numerical groundwater model.

3.7 Hydraulic Head Monitoring

Hydraulic head monitoring was conducted at Westbay Well M11-1257 as part of groundwater sampling, located to the south of Lake B7 and near Lake B5, and at several vibrating wire piezometers installed in the Tiriganiaq underground area to monitor depressurization during mining. Stabilized hydraulic head measurements from Westbay Well M20-2071 near Discovery were unable to be collected in 2020 as the pressures near the well were still recovering from drilling and development at the time of the 2020 data collection.

As part of the FEIS, the approximate direction of groundwater flow between Lake B7 and M11-1257 was estimated using the freshwater heads with a correction for the buoyancy effects, as outlined by Post et al. (2007). These calculations are sensitive on the assumed TDS vs depth profile. For the assumed base TDS profile in the FEIS, which is overall consistent with the updated TDS profile presented in Section 3.4.2, the gradients for the individual ports and Lake B7 are variable but the overall groundwater flow direction between the lake and deep bedrock is downward.

Table 9: Estimated Freshwater Heads, Flow Directions and Gradients

Borehole	Port	Vertical Depth (m)	Freshwater Head at Port (masl)	Freshwater Head at Lake B7 (masl)	Average Density (kg/m^3)	Gradient
M11-1257	2	602.2	65.6	62	1023	0.0174
M11-1257	3	573.7	72	62	1022	0.0047
M11-1257	4	518.7	64.3	62	1020	0.0152
M11-1257	5	448.6	71.5	62	1015	-0.0058
					Average Gradient	0.0079

Note: Gradients calculated between each multi-level port and Lake B7. A positive value indicates a downward gradient. Vertical depths are approximate, due to borehole deviation the actual depth could be +/- 1 m from the tabulated value.

Vibrating wire piezometers have been installed from the Tiriganiaq underground to measure changes in hydraulic head as mining progresses, as presented on Figure 7. The measurements show high variability as result of intersection of permeable features, progressive grouting of the underground development, delays in grouting or sealing of vibrating wire piezometer in the borehole, and challenges / potential malfunction of the dataloggers. Although local temporal variations are difficult to understand in the piezometric data because of the multiple sources of this variability, the long-term trend of these data can be used to understand the extent of depressurization near the underground, particularly at sensors that were installed at the end of 2015, just after the underground extended into the cryopeg.

The data presented on Figure 7 indicates that depressurization has increased in the underground area as the mine development has advanced. Hydraulic heads are generally near the top of the cryopeg and indicate that saturated conditions are generally present near the underground development within the cryopeg and underlying bedrock.

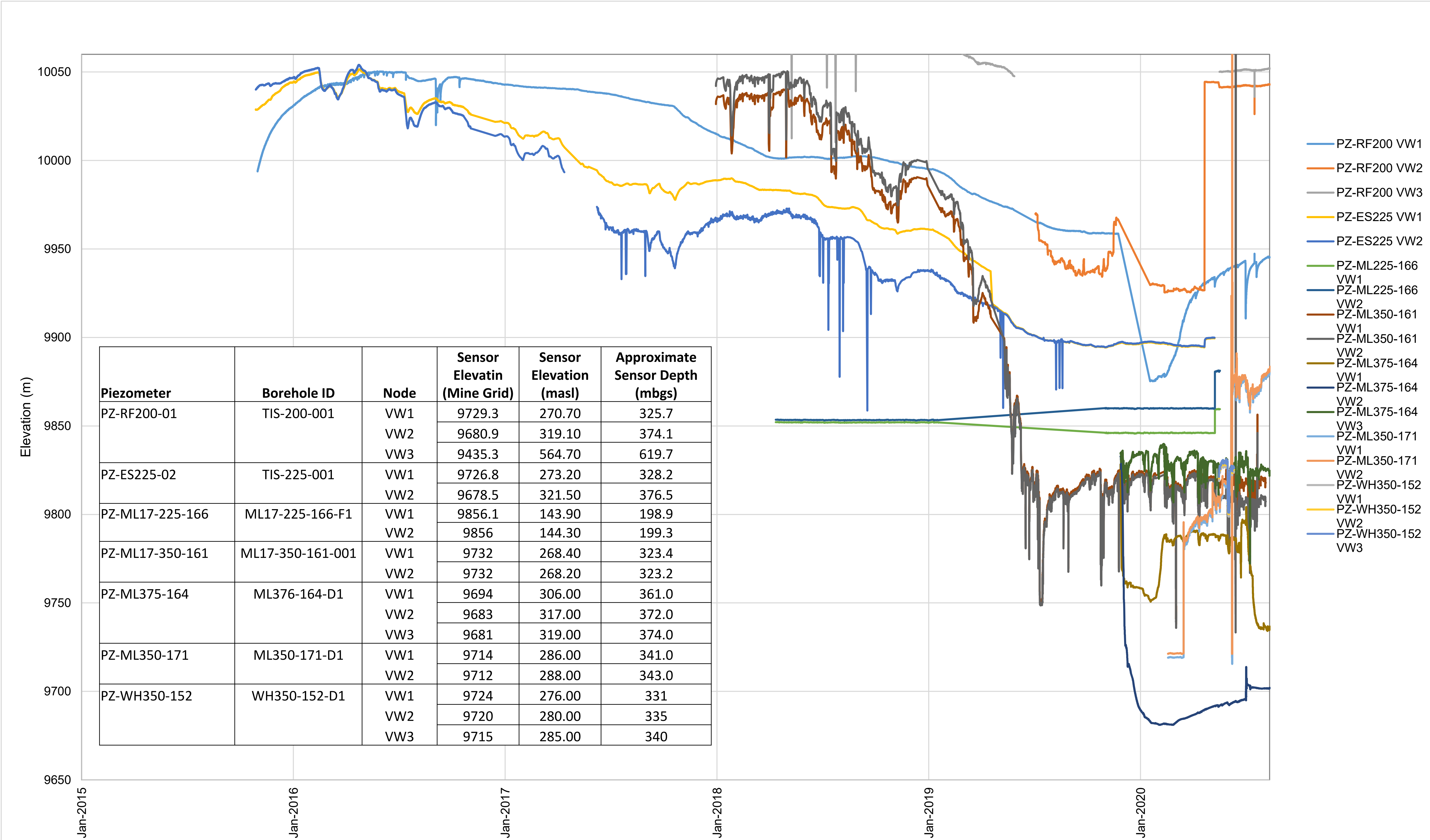

Piezometer	Borehole ID	Node	Sensor Elevatin (Mine Grid)	Sensor Elevation (masl)	Approximate Sensor Depth (mbgs)
PZ-RF200-01	TIS-200-001	VW1	9729.3	270.70	325.7
		VW2	9680.9	319.10	374.1
		VW3	9435.3	564.70	619.7
PZ-ES225-02	TIS-225-001	VW1	9726.8	273.20	328.2
		VW2	9678.5	321.50	376.5
PZ-ML17-225-166	ML17-225-166-F1	VW1	9856.1	143.90	198.9
		VW2	9856	144.30	199.3
PZ-ML17-350-161	ML17-350-161-001	VW1	9732	268.40	323.4
		VW2	9732	268.20	323.2
PZ-ML375-164	ML376-164-D1	VW1	9694	306.00	361.0
		VW2	9683	317.00	372.0
		VW3	9681	319.00	374.0
PZ-ML350-171	ML350-171-D1	VW1	9714	286.00	341.0
		VW2	9712	288.00	343.0
PZ-WH350-152	WH350-152-D1	VW1	9724	276.00	331
		VW2	9720	280.00	335
		VW3	9715	285.00	340

CLIENT
AGNICO EAGLE

CONSULTANT
GOLDER
MEMBER OF WSP

YYYY-MM-DD 2021-11-04
PREPARED HG
DESIGNED HG
REVIEWED JL
APPROVED DC

PROJECT
AGNICO EAGLE MINES LIMITED
MELIADINE EXTENSION
NUNAVUT

TITLE
PRESSURE MONITORING DATA – TIRIGANIAQ UNDERGROUND

PROJECT NO.	PHASE	REV.	FIGURE
20136436	2300	2	7

4.0 CONCEPTUAL HYDROGEOLOGICAL MODEL

Available hydrogeological data collected at the site, together with information collected elsewhere in the Canadian Shield, were used to develop a conceptual understanding of groundwater conditions at the Project. A conceptual hydrogeological model is a pictorial representation of the groundwater regime that organizes and simplifies the site hydrogeology so that it can be readily modelled. The conceptual model must retain sufficient complexity so that the analytical or numerical models developed from it adequately reproduce or simulate the actual components of the groundwater flow system to the degree necessary to satisfy the objectives of the modelling study. During the development of the conceptual model, the main hydrostratigraphic units are defined and characterized, and the dominant groundwater flow patterns are identified both prior to and during mine development. The hydrogeological conceptual model has been developed to describe key features of the hydrogeological regime. The key features include the permafrost depth, hydrostratigraphy/structural geology, groundwater quality, and groundwater flow, all of which are described in below. The baseline conceptual model is described below.

4.1 Permafrost Depth

The base of the permafrost is interpreted as an undulating surface that may vary with latitude, topography and proximity to taliks and it may vary spatially within the overall mine workings. Thermal modelling indicates the depth to permafrost varies between 285 and 430 m depth, with the interpreted depth dependent on the proximity to nearby lakes. Based on the groundwater quality data for the Project (Section 3.4) and thermal modelling (Golder 2021a), the depth to the basal cryopeg where unfrozen groundwater may first be encountered is expected to be approximately 280 to 290 m bgs.

Open taliks are present beneath portions of each of the following lakes near the proposed open pits and undergrounds: Lake B4, Lake B5, Lake B7, Lake A6, Lake A8, Lake CH6 and Lake D4. Based on permafrost limits, open pits in the F Zone, Pump and Discovery, which vary in depth between 70 and 140 mbgs, will be within permafrost. The Wesmeg-North pit is planned to be about 130 m deep and is under a portion of Lake B5 where the models predict the existence of an open talik. The Wesmeg05 pit is planned to be about 120 m deep and is partially under the north side of Lake A8, where the models also predict the existence of an open talik. Each of the underground developments extends into unfrozen bedrock and/or open talik below the lakes.

4.2 Hydrostratigraphy

4.2.1 Geologic Context

The Project is located with the Archaean Rankin Inlet Greenstone Belt, within the Churchill Structural Province of the Canadian Shield (Figure 8). The rocks of the Rankin Inlet Greenstone Belt have been subjected to polyphase deformation events and metamorphism. The rocks consist of a sequence of mafic volcanic rocks, felsic pyroclastic rocks, sedimentary rocks and gabbro sills. The following descriptions are based on information contained in Snowden (2008) and Fingler (2001), as described in the 2014 FEIS (Agnico Eagle 2014a). For a more detailed description of the geology of the Project area, the reader is referred to these reports.

Archean and Proterozoic deformation events have resulted in an alignment of stratigraphy trending in a northwest to southeast direction which defines the Meliadine trend. To the south of the deposits is the Pyke Fault, a major regional fault zone, which extends over several kilometres and is characterized by multiple foliations and regional shear zones.

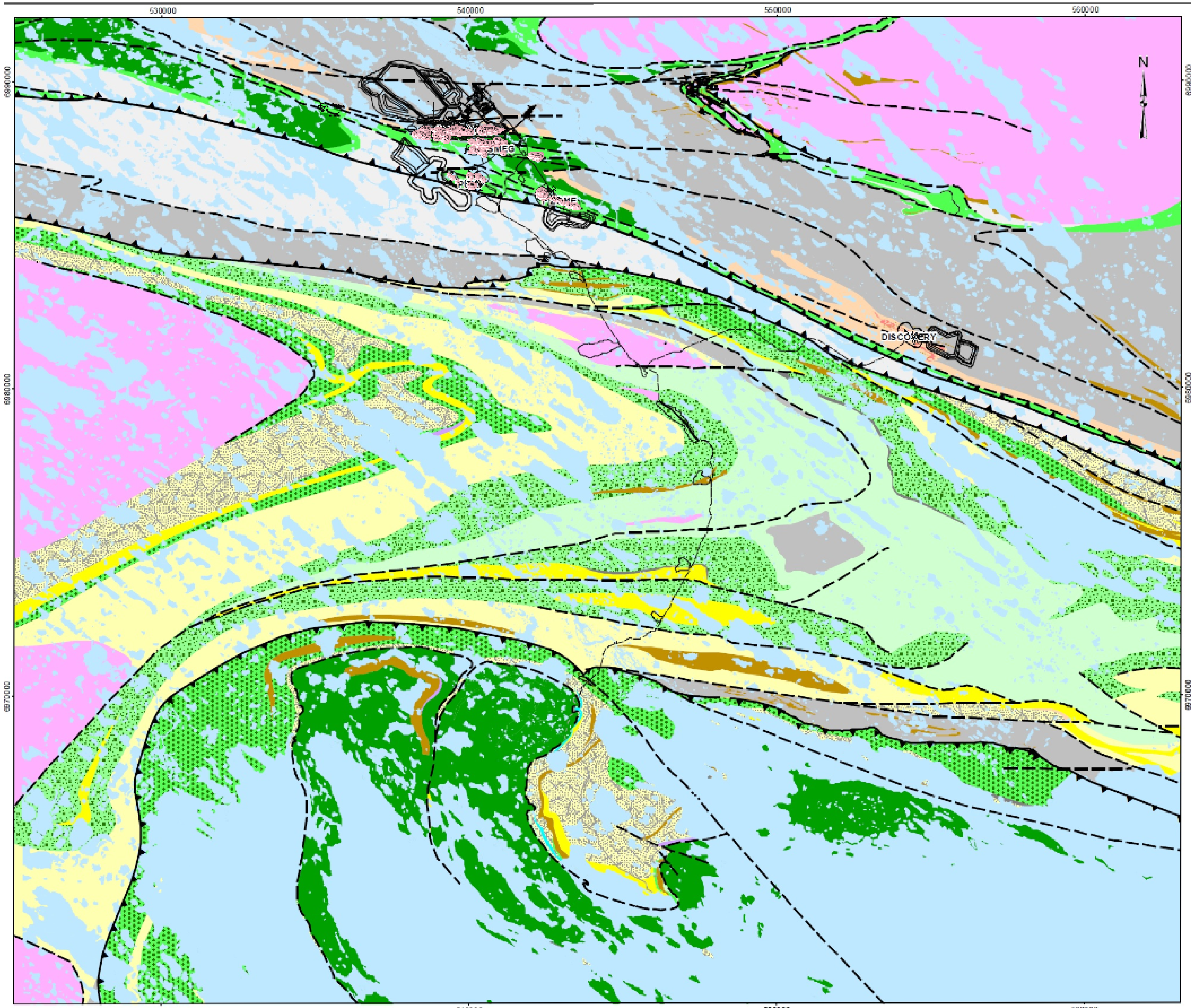

LEGEND

- Proposed Project Infrastructure
- All-weather Access Road (AWAR)
- Road - New
- Road - Existing
- Watercourse
- Waterbody

Regional Geology

- Quartzite
- Quartzite-Siltstone
- Pillowed Mafic Volcanic Rock
- Quartzite-Felsic Volcanic Rock
- Ultramafic Volcanic Rock
- Greywacke-Iron Formation
- Volcanic Rock
- Mafic Volcanic Rock
- Graywacke
- Gabbro
- Granitoid
- Iron Formation
- Andesitic Volcanic Rock
- Carbonated Schist
- Argillite
- Conglomerate
- Dolomite
- Intermediate Volcanic Rock
- Biotite Schist

Major Fault

CLIENT	AGNICO EAGLE
CONSULTANT	GOLDER MEMBER OF WSP
YYYY-MM-DD	2021-11-04
PREPARED	HG
DESIGNED	HG
REVIEWED	JL
APPROVED	DC

PROJECT
AGNICO EAGLE MINES LIMITED
MELIADINE EXTENSION
NUNAVUT

TITLE
REGIONAL GEOLOGY

PROJECT NO.	PHASE	REV.	FIGURE
20136436	2300	2	8

The geology of the Tiriganiaq Deposit consists of greywacke and argillite sediments (Sam Formation), iron formation, and mixed iron formation, greywacke, and siltstone (Upper Oxide Formation) in fault contact with underlying mafic volcanic rocks (Wesmeg Formation). The sequence tends in an east/west direction and dips northward at inclinations greater than about 60 degrees. The stratigraphy is aligned for over 3 km along the mineralized shear direction. The fault contact between the Tiriganiaq and the Wesmeg Formation is referred to as the Lower Fault Zone. A zone of graphitic, mineralized fault gouge (0.5 to 3 m in thickness) commonly occurs over this zone.

The stratigraphy of the F Zone area is dominated by mafic volcanic rocks and the east southeast striking Lower Lean Iron Formation. The deposit area is located north of the Pyke Fault that runs sub-parallel to the Lower Iron Formation. Mineralization of the F Zone is hosted by the Lower Lean Iron Formation and is associated with quartz veins and east striking shear zones.

The stratigraphy of the Discovery area is dominated by a thick package of inter-bedded clastic sedimentary units, chemical sediments (oxide facies iron formations) and minor gabbroic dikes. In the deposit area, the hanging wall to the main gold-bearing iron formation horizon is dominated by a greywacke unit which contains minor interbedded argillaceous units, chemical sediments, and gabbroic dikes. Gold mineralization is generally restricted to a folded and a variably sheared oxide facies iron formation package, which generally consists of banded chert and magnetite horizons with lesser interbedded chlorite-rich beds and chert and minor local interbedded greywacke units. The footwall to the main mineralized iron formation horizon consists of a similar succession of clastic sedimentary units as found in the hanging wall. The footwall stratigraphy is dominated by greywacke, with a more argillaceous interval, approximately 20 to 40 m below the mineralized iron formation.

There appears to be two parts to the Wesmeg gold deposit, a northern and southern part. In the northern part, the stratigraphy strikes east west and dips 65 degrees to the north. The stratigraphy in the southern part strikes northwest southeast and dips 50 degrees to the north. The host Wesmeg Formation is massive to pillowed basalts and interlayered mafic volcaniclastics, with rare gabbro dikes and some interflow sediments consisting of siltstone, mudstone, and minor iron formations.

The stratigraphy in the Pump deposit are strikes northwest southeast and dips 50 degrees to the north. Like the F Zone and Wesmeg deposits, the host rocks at the Pump area are massive to pillowed basalts of the Wesmeg Formation, which are cut by rare gabbro dikes and interflow sediments.

4.2.2 Shallow Bedrock

The shallow bedrock at the site will primarily be within the frozen permafrost except in areas of taliks underlying lakes. In the Canadian Shield, the uppermost zone of bedrock typically has higher hydraulic conductivity (on the order of 10^{-6} to 10^{-7} m/s [Kuchling et al. 2000; DeBeers 2010; Cumberland Resources Ltd. (now Agnico Eagle) 2005]) because of the formation of stress relief joints due to isostatic rebound following glacial retreat. Consequently, the hydraulic conductivity of bedrock to 120 m depth at the Project site has been assumed to be one to two orders of magnitude greater than the values obtained from hydraulic testing at deeper depths (Table 10).

4.2.3 Competent Bedrock

The deep competent bedrock at the Meliadine Project was previously conceptualized as a single hydrostratigraphic unit (Agnico Eagle 2014a). The additional geological interpretation by Agnico Eagle since the 2014 FEIS has enabled a refined interpretation with additional data on the variability of hydraulic conductivity between geologic formations, and data on the storage properties of the bedrock. The current interpretation divides the competent bedrock into two separate units: Mafic Volcanic Rock formations and Sedimentary Rock formations. In past assessments, the Mafic Volcanic Rock Formations have been referred to as Footwall Unit, being in contact with the south side of the Lower Fault and includes the Wesmeg Formation. Agnico Eagle indicates the regional between the Lower Fault and Pyke Fault near Tiriganiaq, Tiriganiaq-Wolf, F Zone, Pump, Wesmeg and Wesmeg-North undergrounds is comprised of the Mafic Volcanic Rock formations. The Mafic rock transitions to Sedimentary Rock Formations towards the Discovery Underground and is also present to the north of the Lower Fault and south of the Pyke Fault, including the area near Tiriganiaq-Wolf and Tiriganiaq undergrounds. The Sedimentary Rock Formations have historically also been referred the Hanging Wall Unit, and contains the Sam, Upper Oxide and Tiriganiaq Formations.

Synthesis of the hydraulic testing results up to the end of 2020, as documented in Section 3.3, indicates that the Mafic Volcanic Rocks has lower hydraulic conductivity than the Sedimentary Rocks (Figure 9) (geometric average of 3×10^{-9} m/s for the Sedimentary Rock formations and 3×10^{-10} m/s for the Mafic Volcanic Rock Formations). Consistent with the 2014 FEIS (Agnico Eagle 2014a) the hydraulic conductivity of the bedrock is assumed to be linearly reduced by an order of magnitude between the top of the basal cryopeg and base of permafrost (zero-degree isotherm). This assumption reflects that this portion of the permafrost which will contain partially unfrozen groundwater due to freezing point depression is expected to have reduced hydraulic conductivity relative to the unfrozen bedrock reflecting the presence of isolated pockets of groundwater within this zone which may be frozen. These frozen zones will result in a decrease in the hydraulic conductivity of the rock compared to that of the entirely unfrozen rock.

The hydraulic conductivity of competent bedrock determined from the hydraulic testing has been assumed to remain constant with depth below 120 m depth. In reality, it is expected that a further reduction in hydraulic conductivity with depth would occur below the depth of testing; however, the rate of this reduction is unknown without further testing.

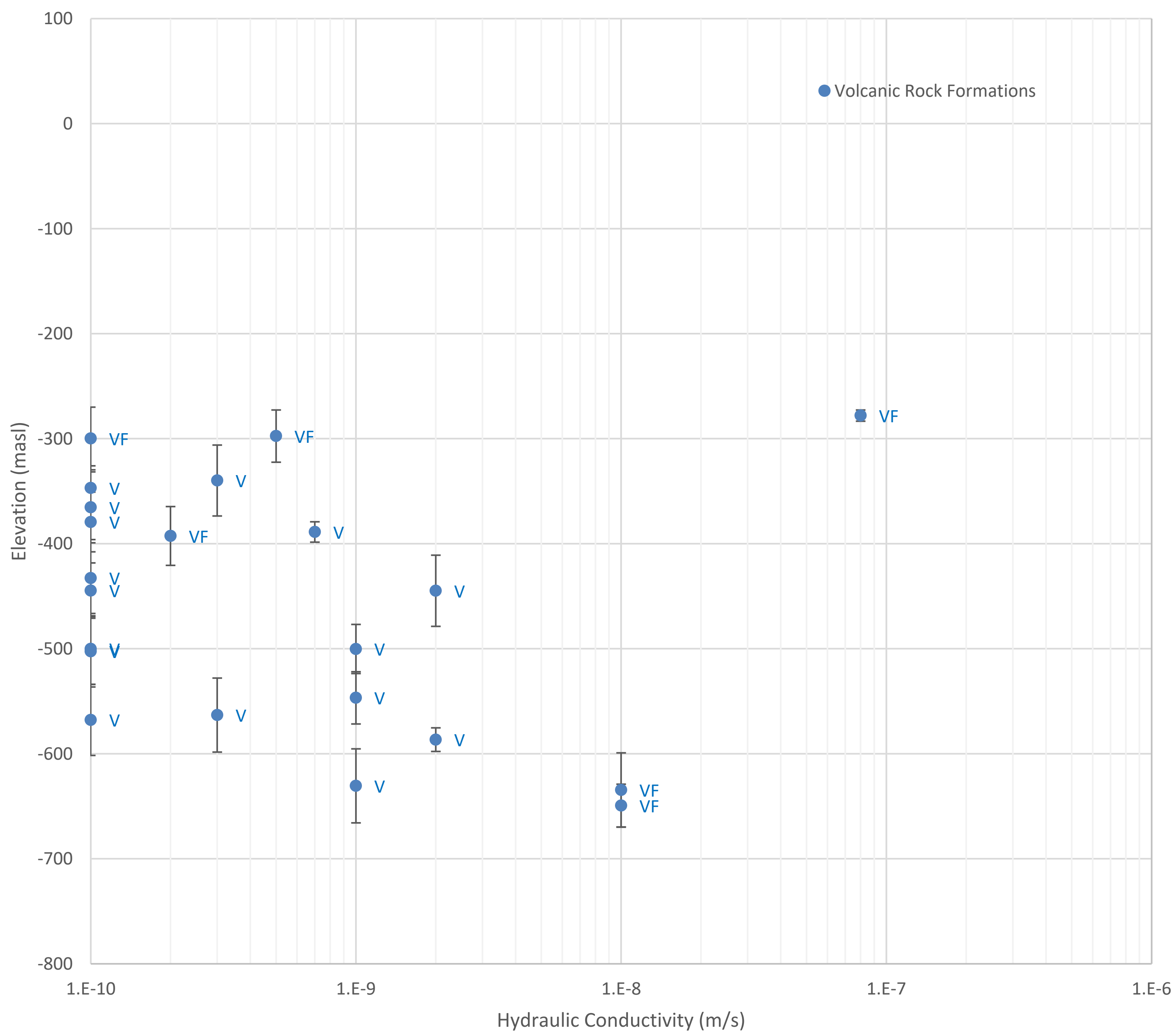

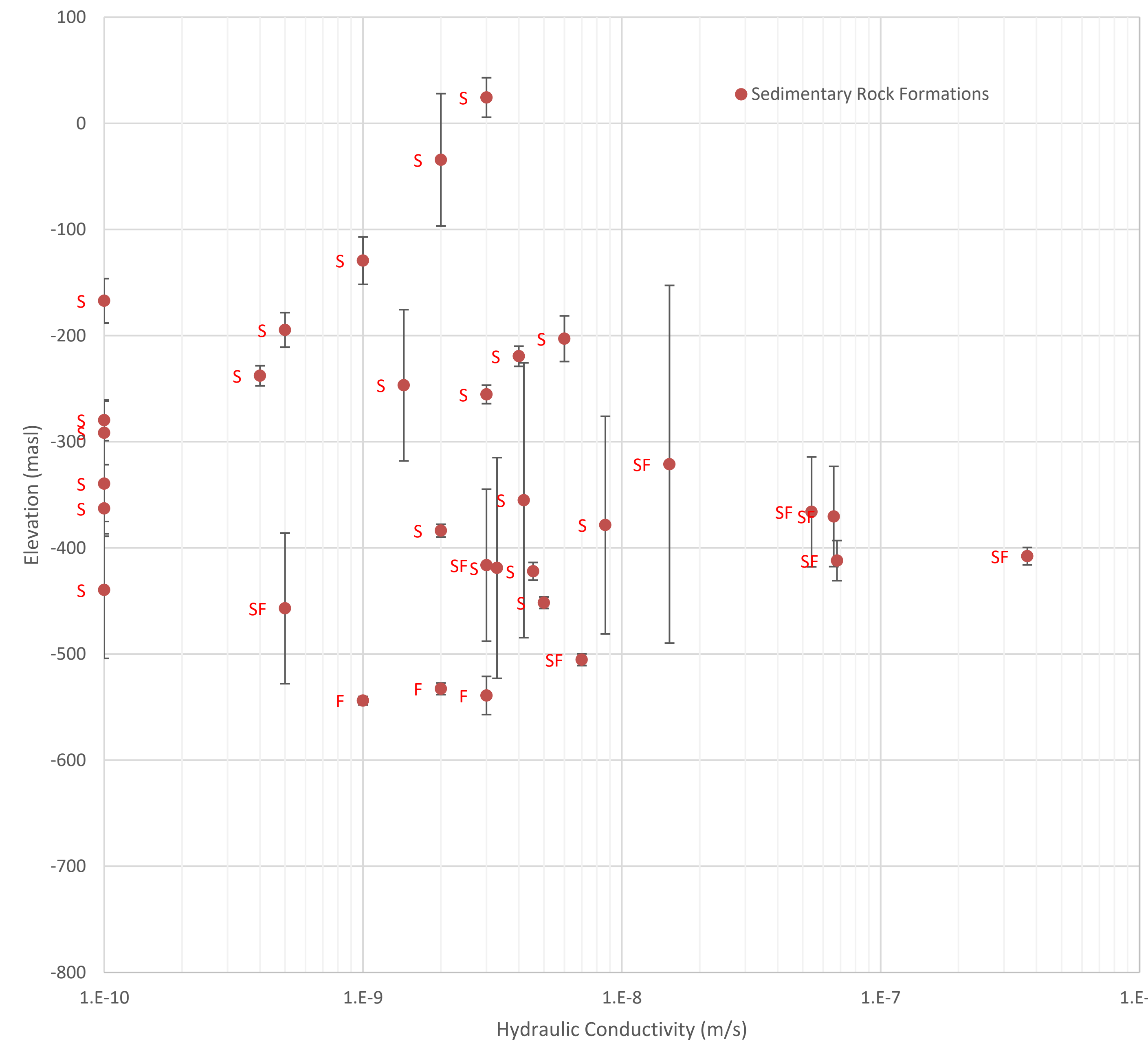

Note: Tests with VF or SF indicate test interval intersected a potential fault. Error bands indicate the interval length.
Tests for the KMS Fault Corridor Not Shown

CLIENT
AGNICO EAGLE

CONSULTANT
GOLDER
MEMBER OF WSP

YYYY-MM-DD	2021-11-04
PREPARED	HG
DESIGNED	HG
REVIEWED	JL
APPROVED	DC

PROJECT
AGNICO EAGLE MINES LIMITED
MELIADINE EXTENSION
NUNAVUT

TITLE
SUMMARY OF AVAILABLE HYDRAULIC CONDUCTIVITY MEASUREMENTS – MAFIC VOLCANIC AND SEDIMENTARY ROCK FORMATIONS

PROJECT NO.	PHASE	REV.	FIGURE
20136436	2300	2	9

4.2.4 Enhanced Permeability Zones Associated with Faults

In crystalline rocks, fault zones may act as groundwater flow conduits, barriers, or a combination of the two in different regions of the fault depending on the direction of groundwater flow and the fault zone architecture (Gleeson and Novakowski 2009). The Lower Fault Zone that forms the fault contact between the Tiriganiaq and the Wesmeg formations, consists of a zone of strongly fractured graphitic and carbonized mudstones infilled with fault gouge in the planned Tiriganiaq underground mine. In the FEIS (Agnico Eagle 2014a), the Lower Fault Zone was assumed to be associated with enhanced permeability, and to have a width of approximately 5 m. Observations made by Agnico Eagle during the advancement of the underground ramp in 2015 were consistent with this interpretation and suggested that the Lower Fault Zone is likely associated with enhanced permeability relative to the surrounding rock. Other faults that have been identified in drilling data or observations in the underground mine, could also be associated with enhanced permeability zones, although there is minimal data to support this. Assuming that they are enhanced permeability zones is a conservative for evaluating inflows to the proposed undergrounds. In the FEIS (Agnico Eagle 2014a), three regional faults were included in the numerical model (Lower Fault, Pyke Fault and North Fault). Of these, only the Lower Fault and Pyke Fault intercept the currently proposed underground developments.

The regional fault passing through the north end of Lake B7, referred to as the North Fault, has been assumed to have a hydraulic conductivity of 1×10^{-7} m/s and width of 5 m, consistent with the previous FEIS (Agnico Eagle 2014a). The Pyke Fault, which is a larger regional feature, has been assumed to have a hydraulic conductivity of 4×10^{-7} m/s and width of 15 m, which is equivalent to a transmissivity of 6×10^{-6} m^2/s. This transmissivity is slightly higher than assumed in the FEIS (5×10^{-6} m^2/s based on an assumed width of 10 m and hydraulic conductivity of 5×10^{-7}). The transmissivity was conservatively increased from the FEIS (Agnico Eagle 2014a) to match the transmissivity at Fault 2, which is the highest packer test result for tested structures. The Lower Fault Zone was assigned a thickness of 5 m and hydraulic conductivity of 1×10^{-7} m/s, which is equivalent to a fault transmissivity of 5×10^{-7} m^2/s. The Lower Fault consists of a zone of graphitic mineralized fault gouge in the Tiriganiaq underground mine area (Agnico Eagle 2014a); the estimated hydraulic conductivity is based on model calibration in 2019 (Golder 2019) and will be reviewed as part of updated model calibration for the Project.

Review of structures in the Project area by Agnico Eagle identified 17 additional faults that have been incorporated into the conceptual hydrostratigraphy. The additional structures are generally located between the Lower Fault and Pyke Fault within the Mafic Volcanic Rock formations and range in thickness between 2 and 6 m. An exception is the KMS fault corridor, located in the sedimentary rock formations to the north of the Lower Fault at the Tiriganiaq Underground. This corridor is a wider zone of rock located between the KMS fault and Lower Fault that is associated with poor rock quality.

In the Tiriganiaq area, flow recession tests conducted in 2020 indicated the KMS corridor or zone of broken rock between the KMS Fault and the Lower Fault has a hydraulic conductivity of 4×10^{-7} m/s, based on the geometric average of the long-term flow recession testing. These data indicate that the corridor has some compartmentalization and is not uniformly permeable throughout, as indicated by the calculated diffusivity values.

Testing of the other discrete faults has occurred in the Tiriganiaq and Discovery area in RM-175, Fault A and Fault 2. In the exploratory ramp, an enhanced permeability zone associated with the interpreted RM-175 was encountered. A hydraulic conductivity of 5×10^{-8} m/s was assigned to the RM-175 based on the observed inflow to the ramp from this structure. This value is similar to but slightly higher than the estimate from packer testing at TIS-200-002.

Fault A hydraulic conductivity was estimated from recession tests and packer tests to range between 4 x 10^{-8} to 2 x 10^{-7} m/s. The maximum test value of 2 x 10^{-7} m/s was assigned to the fault. Fault 2 was also estimated to have a hydraulic conductivity of 2 x 10^{-7} m/s, based on an estimated packer test transmissivity of 5 x 10^{-6} m^2/s and an observed fault width at the borehole of approximately 12 m. Considering the testing undertaken to date and potential variability across the length of each fault, each of the nonregional faults, other than RM175 that was intersected by the under-ground ramp, KMS corridor, and Fault A that have site specific testing, have been assumed to have a transmissivity of 5 x 10^{-6} m^2/s, which is the maximum of the packer testing results over a fault. The lateral extents of the faults near the underground developments have not been mapped and therefore the faults were conservatively extended approximately 2.5 km from intersected undergrounds. This is considered conservative since the permeability and width of a fault zone can be heterogeneous along strike (Gleeson and Novakowski 2009) resulting potentially in zones of greater hydraulic conductivity along strike over short distances; whereas over longer distances the presence of zones infilled with fault gouge will act to decrease hydraulic connectivity along strike. Observations during testing at Fault A is indicative of this variability.

4.2.5 Estimated Hydraulic Properties

Table 10 and Table 11 present a summary of the hydrostratigraphic units and their estimated hydraulic properties based on the hydraulic testing presented in this report and based on published data for similar lithologies.

Table 10: Estimated Hydraulic Properties - Competent Bedrock

Hydrostratigraphic Unit	Depth Interval (m)	Hydraulic Conductivity[(a)] (m/s)	Specific Storage[(b)] (1/m)	Effective Porosity[(c)] (-)
Shallow Rock	0 to 60	3×10^{-7}	1×10^{-6}	0.001
	60 to 120	3×10^{-8}	1×10^{-6}	0.001
Sedimentary Rock Formations(d)	120 to 1500	3×10^{-9}	2×10^{-6}	0.001
Mafic Volcanic Rock Formations(d)	120 to 1500	3×10^{-10}	2×10^{-7}	0.001

Note: Hydraulic conductivity within the unfrozen permafrost zone is assumed to be lower than in the deeper unfrozen rock. Linearly decreasing hydraulic conductivity with temperature is assumed within this zone with a full order of magnitude decrease assumed at the top of the basal cryopeg, and hydraulic conductivity equivalent to unfrozen rock at the bottom of the basal cryopeg.

a) Parameter values based on in-situ testing and 2019 Model Calibration (Golder 2020)

b) Parameter values based on in-situ testing and values documented in literature (Maidment 1992; Stober and Bucher 2007).

c) Values consistent with literature values (Guimerà J, Carrera J. 2000).

Table 11: Estimated Hydraulic Properties – Enhanced Permeability Zones

Hydrostratigraphic Unit	Depth Interval[e] (m)	Thickness[d] (m)	Hydraulic Conductivity[a] (m/s)	Specific Storage[b] (1/m)	Effective Porosity[c] (-)	Source of Transmissivity[a] (T) Estimate
Lower Fault Zone	0 to 1000	5	1×10^{-7}	2×10^{-7}	0.001	2019 Calibration
RM-175	0 to 1000	5	5×10^{-8}	2×10^{-7}	0.001	In-Situ and 2019 Calibration
KMS Fault Corridor	0 to 1000	100	4×10^{-7}	2×10^{-7}	0.001	In-Situ Testing
North Fault	0 to 1000	5	1×10^{-7}	2×10^{-7}	0.001	Assumed T Equal to Fault 2
A	0 to 1000	6	1×10^{-6}	2×10^{-7}	0.001	Assumed T Equal to Fault 2
B	0 to 1000	5	1×10^{-6}	2×10^{-7}	0.001	Assumed T Equal to Fault 2
C	0 to 1000	3	2×10^{-6}	2×10^{-7}	0.001	Assumed T Equal to Fault 2
D	0 to 1000	5	1×10^{-6}	2×10^{-7}	0.001	Assumed T Equal to Fault 2
Pyke Fault	0 to 1000	15	4×10^{-7}	2×10^{-7}	0.001	Assumed T Equal to Fault 2
AP0	0 to 1000	3	2×10^{-6}	2×10^{-7}	0.001	Assumed T Equal to Fault 2
ENE2	0 to 1000	5	1×10^{-6}	2×10^{-7}	0.001	Assumed T Equal to Fault 2
ENE3	0 to 1000	3	2×10^{-6}	2×10^{-7}	0.001	Assumed T Equal to Fault 2
UM2	0 to 1000	6	1×10^{-6}	2×10^{-7}	0.001	Assumed T Equal to Fault 2
NW1	0 to 1000	5	1×10^{-6}	2×10^{-7}	0.001	Assumed T Equal to Fault 2
WNW1	0 to 1000	3	2×10^{-6}	2×10^{-7}	0.001	Assumed T Equal to Fault 2
WNW2	0 to 1000	3	2×10^{-6}	2×10^{-7}	0.001	Assumed T Equal to Fault 2
UAU2	0 to 1000	2	3×10^{-6}	2×10^{-7}	0.001	Assumed T Equal to Fault 2
Fault 1	0 to 1000	5	1×10^{-6}	2×10^{-7}	0.001	Assumed T Equal to Fault 2
Fault 2	0 to 1000	5	1×10^{-6}	2×10^{-7}	0.001	In-Situ Testing
Fault 3	0 to 1000	5	1×10^{-6}	2×10^{-7}	0.001	Assumed T Equal to Fault 2

a) Hydraulic conductivity within the unfrozen permafrost zone is assumed to be lower than in the deeper unfrozen rock. Linearly decreasing hydraulic conductivity with temperature is assumed within this zone with a full order of magnitude decrease assumed at the top of the basal cryopeg, and hydraulic conductivity equivalent to unfrozen rock at the bottom of the basal cryopeg.

b) Assumed parameter in consideration of competent bedrock testing.

c) Values consistent with literature values (Guimerà J, Carrera J. 2000).

d) Width of structures estimated by Agnico Eagle from review of borehole records.

e) Where fault hydraulic conductivity is less than shallow rock, the fault was excluded from 0 to 60 m depth interval. Where fault hydraulic conductivity is greater than shallow rock, fault was be included within 0 to 60 m depth interval.

4.3 Conceptual Groundwater Flow – Pre-Mining

The conceptual hydrogeological model for pre-disturbance conditions is presented in Figure 10, with interpreted regional flow directions presented on Figure 1. In areas of continuous permafrost there are generally two groundwater flow regimes; a deep groundwater flow regime beneath the base of the permafrost and a shallow flow regime located in an active (seasonally thawed) layer near ground surface. Permafrost reduces the hydraulic conductivity of the rock by several orders of magnitude (McCauley et al. 2002; Burt and Williams 1976). The shallow groundwater flow regime, therefore, has little to no hydraulic connection with the groundwater regime located below the permafrost. Taliks (areas of unfrozen ground surrounded by permafrost) may be present in the permafrost in areas underlying lakes. Depending on lake size, depth, and thermal storage capacity, the taliks beneath lakes may fully penetrate the permafrost layer resulting in an open talik providing a hydraulic connection between surface water and the deep groundwater flow regime.

The elevations of the lakes underlain by open taliks provide the driving force for deep groundwater flow. The presence of thick permafrost beneath land masses results in negligible recharge to the deep groundwater flow regime from these areas. Consequently, recharge to the deep groundwater flow regime is predominantly limited to areas of taliks beneath large, surface water bodies. Generally, deep groundwater will flow from higher-elevation lakes to lower-elevation lakes. Groundwater beneath the permafrost is also influenced by density differences due to the upward diffusion of deep-seated brines (density-driven flow).

The Westbay multi-level monitoring system that was installed in borehole M11-1257 is situated near Lake B5 between Lakes B7 and D7. Each of these lakes are predicted to be connected to the deep groundwater flow regime through open taliks. The multi-level sampling intervals in the Westbay system were installed beneath permafrost in the deep groundwater flow regime at vertical depths ranging from approximately 440 to 640 m below ground surface. Due to the inclination of this installation, these ports are located beneath Lake B5. Groundwater pressures and quality collected from the Westbay installation are considered representative of the deep groundwater flow regime, which is expected to be driven by the hydraulic gradients between Lakes B7 and D7 and Meliadine lake, and by density gradients.

Groundwater pressures recorded in the intervals of the Westbay system, and the approximate direction of vertical groundwater flow estimated using these recorded pressures (freshwater heads) corrected for buoyancy effects due to density contrasts were presented in the Golder (2021b; 2021c). Results of this analysis indicated that relative to Lake D7 (Lake Elevation of 62 m), a general downward groundwater flow direction is observed, which would be consistent with flow from high elevation lakes (Lake D7) to low elevation lakes (Lake B5 at 58 masl or Lake D7 at 57 masl). Relative to Lake B5, a variable vertical groundwater flow direction was observed. This may reflect that Lake B5 is both a recharge and discharge boundary given the relative elevation of the surrounding lakes.

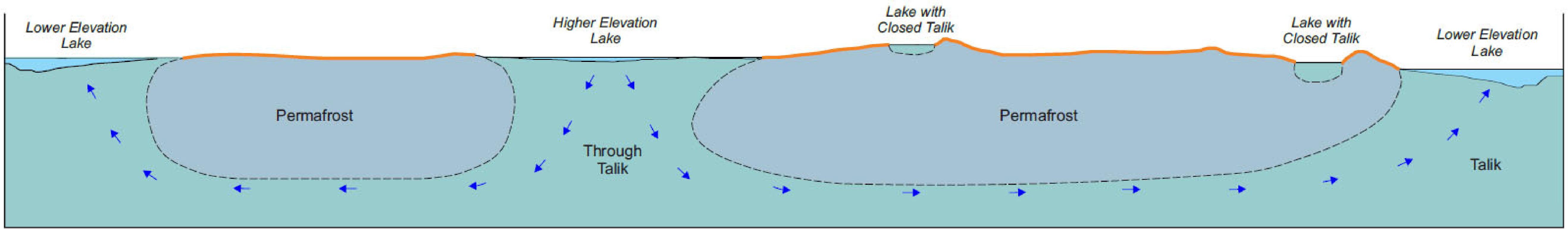

CROSS SECTION

Schematic Only
Not to Scale

LEGEND

- Conceptual Groundwater Flow Direction
- Active Layer

CLIENT: AGNICO EAGLE		PROJECT: AGNICO EAGLE MINES LIMITED MELIADINE EXTENSION NUNAVUT	
CONSULTANT: GOLDER MEMBER OF WSP	YYYY-MM-DD: 2021-11-04	TITLE: **CONCEPTUAL PERMAFROST AND GROUNDWATER FLOW MODEL – BASELINE CONDITIONS**	
	PREPARED: HG		
	DESIGNED: HG		
	REVIEWED: JL		
	APPROVED: DC	PROJECT NO. 20136436 / PHASE 2300 / REV. 2	FIGURE 10

4.4 Conceptual Groundwater Flow – Existing Conditions

Groundwater inflows are presently intercepted at the Tiriganiaq Undergound, where mining has extended into the basal cryopeg and/or into the unfrozen rock below lakes with open taliks. In September of 2015, the mine development extended to approximately 280 m depth which corresponds to the estimated top of the basal cryopeg. Groundwater inflows were low (approximately 15 m^3/day in the fourth quarter of 2015) but have since increased on an average of between 200 and 300 m^3/day in 2020. Groundwater inflows are mitigated by active grouting which locally reduces the effective hydraulic conductivity of structures adjacent to the development.

Each underground and open pit within the unfrozen rock will act as a sink for groundwater flow, with water induced to flow through the bedrock to the underground mine workings once the mine has advanced into and below the basal cryopeg, or into the open talik below a lake. These include:

- Open Pits: Wesmeg-North and Wesmeg05
- Undergrounds: Tiriganaiq, Tiriganiaq-Wolf, Pump, F Zone, Wesmeg, Wesmeg-North, Discovery

At Tiriganiaq, local depressurization of over 350 m has been observed at piezometers installed near the underground. Further depressurization is expected at other undergrounds and open pits as they develop.

Outside of Wesmeg-North and Wesmeg05, none of the other open pits are interpreted to intersect the cryopeg or deep groundwater regime below the permafrost. Portions of the pits may intersect small layers and may have limited unfrozen groundwater within closed taliks.

5.0 CLOSURE

The reader is referred to the Study Limitations, which follows the text and forms an integral part of this report.

We trust the above meets your present requirements. If you have any questions or require additional information, please contact the undersigned.

Golder Associates Ltd.

Jennifer Levenick, M.Sc., P.Eng.
Associate, Senior Hydrogeologist

Don Chorley, M.Sc., P.Geo
Senior Hydrogeology Specialist

JL/DC/pls/hp

PERMIT TO PRACTICE
GOLDER ASSOCIATES LTD.
Signature ____________
Date 2 December 2021
PERMIT NUMBER: P 049
NT/NU Association of Professional Engineers and Geoscientists

Golder and the G logo are trademarks of Golder Associates Corporation

https://golderassociates.sharepoint.com/sites/120710/project files/6 deliverables/working/20136436-855-r-rev3-hydroexistingconditions/20136436-855-r-existingconditionsreport-rev3.docx

REFERENCES

Agnico Eagle Ltd. (Agnico Eagle) 2014a. Volume 7.0 Freshwater Environmental, Final Environmental Impact Statement (FEIS) – Meliadine Gold Project. Report Number Doc 314-1314280007 Ver. 0. April 2014

Agnico Eagle 2014b. Meliadine – Westbay Well 2014 Sampling Campaign. 22 July 2014.

Agncio Eagle 2014c. Follow-Up of Deep Ground Thermistor Cables at Meliadine – Compilation of the Data from 1998 to 2014. Revision A. October 2014.

Blowes, D.W. and M.J. Logsdon. 1997. Diavik Geochemistry 1996-1997 Baseline Report. Prepared for Diavik Diamond Mines Inc.

Burt, T.P. and P.J. Williams. 1976. Hydraulic Conductivity in Frozen Soils, Earth Surface Processes, Volume 1, John Wiley, pp. 349-360.

Cumberland Resources Ltd., 2005. Meadowbank Gold Project Mine Waste and Water Management. October 2005.

De Beers (De Beers Canada Inc.) 2010. Environmental Impact Statement for the Gahcho Kue Project. Volumes 1, 2, 3a, 3b, 4, 5, 6a, 6b, 7 and Annexes A through N. Submitted to Mackenzie Valley Environmental Impact Review Board. December 2010.

Dominion Diamond (Dominion Diamond Ekati Corporation). 2014. Developer's Assessment Report Hydrogeology Baseline Report Annex IX. September 2014.

Dyke, A.S., A. Moore, and L. Robertson. 2003. Deglaciation of North America, Geological Survey of Canada Open File 1574.

Fingler, J.F. 2001. 2000 Geological, geochemical, geophysical and diamond drilling report for the Fay 1, Fay 2 and Felsic 1 Concessions, Meliadine East Property. NTI Assessment Report for Cumberland Resources ltd. On behalf of the Meliadine East Joint Venture.

Frape, S.K. and P. Fritz. 1987. Geochemical Trends for Groundwaters from the Canadian Shield; in Saline Water and Gases in Crystalline Rocks. Editors: Fritz, P. And Frape, S.K. Geological Association of Canada Special Paper 33.

Gleeson, T. and K.S. Novakowski. 2009. Identifying watershed barriers to groundwater flow: Lineaments in the Canadian Shield. Geological Society of America Bulletin, 121:333-347.

Golder Associates Ltd. 2004. Predictions of Brackish Water Upwelling in Open Pits, Meadowbank Project Nunavut.

Golder Associates Ltd. 2009. Hydrogeologic Investigation Program – Meliadine Project. Doc. 039. Golder Associates Ltd. 6 November 2009.

Golder Associates Ltd. 2011. Appendix 7.2-C 2009 and 2011 Hydrogeological Testing and Groundwater Sampling Programs. Doc 436-1314280007 Ver 0

Golder Associates Ltd. 2014. SD 6-1 Permafrost Thermal Regime Baseline Studies – Meliadine Golder Project Nunavut. September 25 2012. Report Number: Doc 225-1013730076 Ver.0.

Golder Associates Ltd. 2016. Factual Report for Meliadine Project, Nunavut. Hydrogeological Investigation in Support of the Underground Mine Development at Tiriganiaq. Golder Doc. 547-1416135 Ver 0. 18 March 2016.

Golder Associates Ltd. 2021a. Meliadine Extension – 2020 Thermal Assessment. Golder Doc. 20136436-815-R-Rev1. November 2021.

Golder Associates Ltd. 2021b. Westbay Monitoring Well System M20-3071 Groundwater Quality Assessment Meliadine Extension. Golder Doc. 20136436-817-R-Rev1. November 2021.

Golder Associates Ltd. 2021c. Installation of Westbay Monitoring Well System M20-3071 Meliadine Extension . Golder Doc. 20136436-820-R-Rev2. November 2021.

Kuchling, K., D. Chorley and W. Zawadzki. 2000. Hydrogeological modelling of mining operations at the Diavik Diamonds Project. In Proceedings of the Sixth International Symposium on Environmental Issues and Waste Management in Energy and Mineral Production, University of Calgary, Calgary AB.

McCauley, C.A, D.M. White, M.R. Lilly, and D.M. Nyman. 2002. A comparison of hydraulic conductivities, permeabilities and infiltration rates in frozen and unfrozen soils. Cold Regions Science and Technology 34(2002). PP. 117-125.Ophori, D.U., and Chan, T. 1994. Regional Groundwater Flow in the Atikokan Research Area; Simulation of 18O and 3H Distributions. AECL-11083. Manitoba.

Post, B., Kooi, H. and Simmons, C., 2007. Using hydraulic head measurements in variable-density ground water flow analyses. Ground Water, 45(6): 664-671.

R.L.&L. (R.L.&L. Environmental Services Ltd. 199. Meliadine West Baseline Aquatic Studies: 1988 Data Report. Prepared for WMC International Ltd.

Séguin, A. 1995. Origin of saline groundwaters in Torbolton Ward, Eastern Ontario. Master of Science Thesis, Department of Earth Sciences, University of Ottawa, Ontario.

Snowden 2008. Comaplex Minerals Corp. Report on Tiriganiaq Gold Deposit, Nunavut – Resource Update January 2018.

Stotler, R, S.K. Frape, T. Ruskeeniemi, P. Pitkänen, and D.W. Blowes. 2012. The interglacial–glacial cycle and geochemical evolution of Canadian and Fennoscandian Shield groundwaters. Geochimica et Cosmochimica Acta 76 (2012): 45–67.

STUDY LIMITATIONS

Golder Associates Ltd. (Golder) has prepared this document in a manner consistent with that level of care and skill ordinarily exercised by members of the engineering and science professions currently practising under similar conditions in the jurisdiction in which the services are provided, subject to the time limits and physical constraints applicable to this document. No warranty, express or implied, is made.

This document, including all text, data, tables, plans, figures, drawings and other documents contained herein, has been prepared by Golder for the sole benefit of Agnico Eagle Mines Limited. It represents Golder's professional judgement based on the knowledge and information available at the time of completion. Golder is not responsible for any unauthorized use or modification of this document. All third parties relying on this document do so at their own risk.

The factual data, interpretations, suggestions, recommendations and opinions expressed in this document pertain to the specific project, site conditions, design objective, development and purpose described to Golder by Agnico Eagle Mines Limited and are not applicable to any other project or site location. In order to properly understand the factual data, interpretations, suggestions, recommendations and opinions expressed in this document, reference must be made to the entire document.

This document, including all text, data, tables, plans, figures, drawings and other documents contained herein, as well as all electronic media prepared by Golder are considered its professional work product and shall remain the copyright property of Golder. Agnico Eagle Mines Limited may make copies of the document in such quantities as are reasonably necessary for those parties conducting business specifically related to the subject of this document or in support of or in response to regulatory inquiries and proceedings. Electronic media is susceptible to unauthorized modification, deterioration and incompatibility and therefore no party can rely solely on the electronic media versions of this document.

APPENDIX A

Location of Thermal Model Cross-Sections (from Golder 2021)

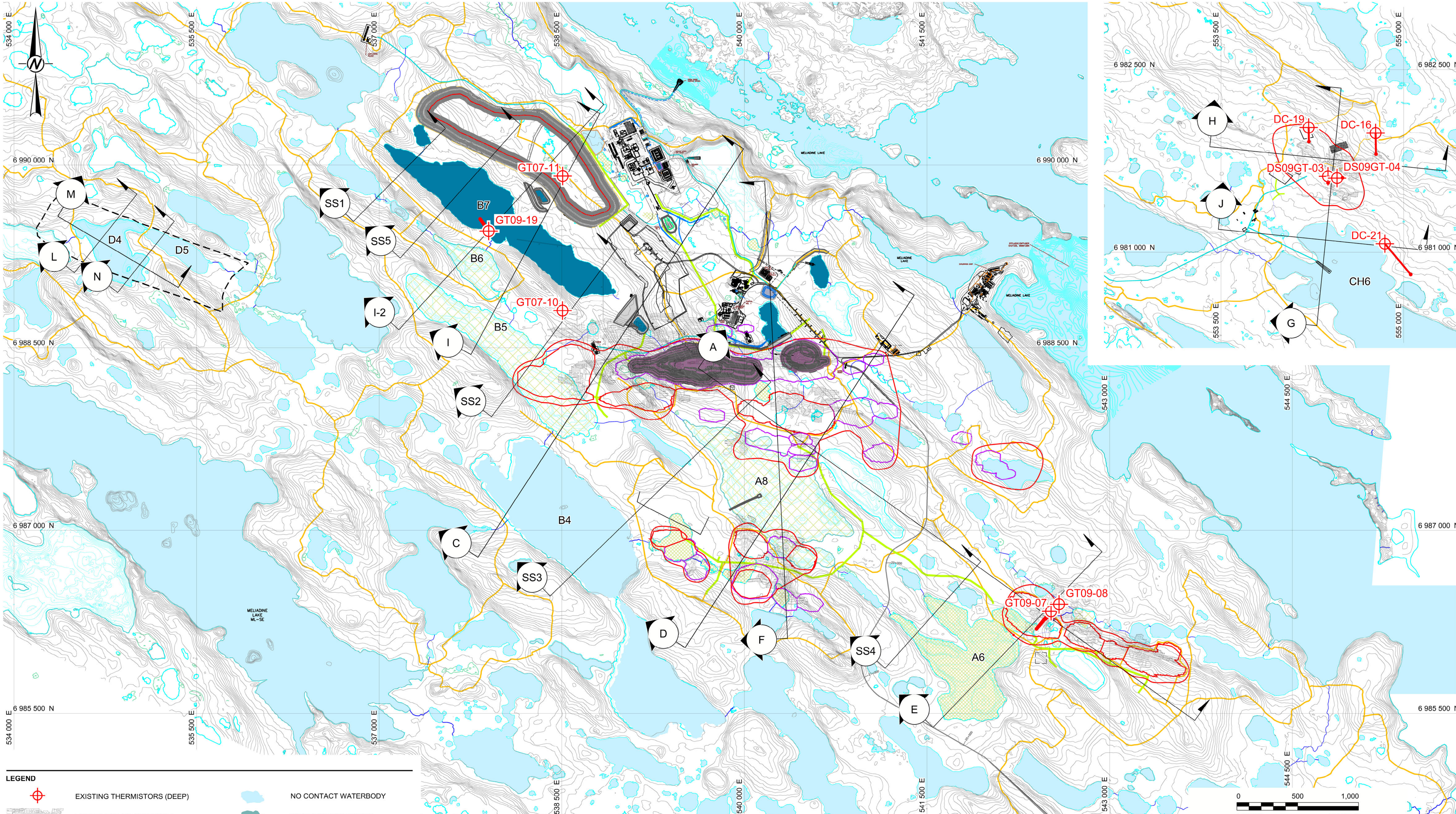

LEGEND

- EXISTING THERMISTORS (DEEP)
- UNDERGROUND WORKINGS
- CATCHMENT BOUNDARY
- PLOM 2020 PIT DESIGN LIMIT
- PERMITTING BOUNDARY
- ORE BODY
- HAUL ROAD
- TIRIGANIAQ-NORTH EXTENTS
- NO CONTACT WATERBODY
- CONTACT WATERBODY
- WATER COLLECTION POND
- DRAINED LAKE AREA

REFERENCE

1. BASE MAP OBTAINED FROM AGNICO EAGLE CAD
   FILE: OPTION E_PLOM2020_final_V4.dwg, DATE RECEIVED: 2020-03-20
2. 2020 EXPLORATION BOREHOLES PROVIDED BY AEM EXCEL
   FILE Discovery_CONV_DISCO_2020_collar, DATE RECEIVED: 2020-04-07

NOTES

1. INSTALLATION OF A NEW DEEP THERMISTOR WILL ALSO BE REQUIRED FOLLOWING SELECTION OF THE WESTBAY WELL LOCATION.
2. INSTALLATION OF NEW SHALLOW THERMISTORS BETWEEN THE LAKE CH6 AND MELIADINE LAKE IS ALSO RECOMMENDED.

CLIENT	AGNICO EAGLE
PROJECT	MELIADINE EXTENSION
CONSULTANT	GOLDER MEMBER OF WSP
YYYY-MM-DD	2021-11-04
DESIGNED	ZM
PREPARED	AF
REVIEWED	FJ
APPROVED	JL
TITLE	THERMAL MODEL CROSS SECTION LOCATIONS
PROJECT NO.	20136436
PHASE/TASK	2400/2405
REV.	0
FIGURE	A-1

GOLDER
MEMBER OF WSP

golder.com